The Astrophysical Journal Supplement Series, 175:462–484, 2008 April

SPATIALLY RESOLVED SPECTROSCOPY OF COMA CLUSTER EARLY-TYPE GALAXIES. IV. COMPLETING THE DATA SET[1]

E. M. Corsini
Dipartimento di Astronomia, Università di Padova, vicolo dell'Osservatorio 3, 35122 Padova, Italy; enricomaria.corsini@unipd.it

G. Wegner[2]
Department of Physics and Astronomy, 6127 Wilder Laboratory, Dartmouth College, Hanover, NH 03755-3528; gaw@bellz.dartmouth.edu

R. P. Saglia
Max-Planck-Institut für extraterrestrische Physik, Giessenbachstraße, D-85748 Garching, Germany; saglia@mpe.mpg.de

J. Thomas and R. Bender
Max-Planck-Institut für extraterrestrische Physik, Giessenbachstraße, D-85748 Garching, Germany, and Universitäts-Sternwarte München, Scheinerstraße 1, D-81679 München, Germany; jthomas@mpe.mpg.de, bender@mpe.mpg.de

and

D. Thomas
Institute of Cosmology and Gravitation, Mercantile House, Hampshire Terrace, University of Portsmouth, Portsmouth PO1 2EG, UK; daniel.thomas@port.ac.uk

Received 2007 July 10; accepted 2007 October 1

ABSTRACT

The long-slit spectra obtained along the minor axis, offset major axis, and diagonal axis are presented for 12 E and S0 galaxies of the Coma Cluster drawn from a magnitude-limited sample studied before. The rotation curves, velocity dispersion profiles, and the H_3 and H_4 coefficients of the Hermite decomposition of the line-of-sight velocity distribution are derived. The radial profiles of the Hβ, Mg, and Fe line strength indices are measured too. In addition, the surface photometry of the central regions of a subsample of four galaxies recently obtained with the *Hubble Space Telescope* is presented. The data will be used to construct dynamical models of the galaxies and study their stellar populations.

Subject headings: galaxies: abundances — galaxies: elliptical and lenticular, cD — galaxies: formation — galaxies: kinematics and dynamics — galaxies: stellar content

Online material: machine-readable tables

1. INTRODUCTION

This is the fourth of a series of papers aimed at investigating the stellar populations and the kinematics of early-type galaxies in the Coma Cluster. Spanning about 4 dex in the observed radial variation of the surface density of cluster members (e.g., Kent & Gunn 1982), the Coma Cluster is the ideal place to investigate these galaxy properties as a function of the environmental density in order to test the theories for galaxy formation and evolution.

The sample of 35 E and S0 galaxies of the Coma Cluster is presented in the first paper of the series (Mehlert et al. 2000, hereafter Paper I) along with the photometry and long-slit spectroscopy along their major axis. From these spectra the rotation curves, velocity dispersion profiles, and the H_3 and H_4 coefficients of the Hermite decomposition of the line-of-sight velocity distribution (LOSVD) were measured out to 1–3 effective radii with high signal-to-noise ratio (S/N). Moreover, the radial profiles of the Hβ, Mg, and Fe line strength indices were measured too. Subsequently, the spectroscopic database was complemented with the long-slit spectra obtained along the minor axis, an offset axis parallel to the major one, and one diagonal axis for 10 objects (Wegner et al. 2002, hereafter Paper II).

The central values and major-axis logarithmic gradients for the line strength indices were derived by Mehlert et al. (2003, hereafter Paper III). This allowed the estimation of the average ages, metallicities, and [α/Fe] ratios in the center and at the effective radius by using stellar population models with variable element abundance ratios from Thomas et al. (2003). There is a dichotomy among the population of S0 galaxies. Some of them are dominated by old stellar populations and are indistinguishable from E galaxies. The remaining ones host very young stellar populations; hence, they must have experienced relatively recent star formation episodes. Most massive galaxies had the shortest star formation timescales and were the first to form. The absence of age gradients implies that the stellar populations at different radii formed at a common epoch. The [α/Fe] enhancement is not restricted to galaxy centers but is a global phenomenon. Finally, negative metallicity gradients were measured to be significantly flatter than what is expected from gaseous monolithic collapse models. This suggests the importance of mergers in the galaxy formation history.

Here the spectroscopic database of Papers I and II is completed with the long-slit spectra obtained along the minor axis,

[1] Based on data collected with the Hobby-Eberly Telescope and the 2.4 m Hiltner Telescope.

[2] Visiting Astronomer, MDM Observatory, Kitt Peak, Arizona, operated by a consortium of Dartmouth College, the University of Michigan, Columbia University, the Ohio State University, and Ohio University.

offset major axis, and one diagonal axis for another 12 objects. As done in Paper II, these galaxies were selected from the sample of Paper I as the objects with the most extended and precise major-axis kinematics and therefore best suited for dynamical modeling, balancing between the number of E and S0 galaxies. Moreover, the surface photometry of the central regions of a subsample of four galaxies recently obtained with *Hubble Space Telescope* (*HST*) is presented.

The data shown here and in Paper I will allow the study of the stellar population gradients for a large number of early-type galaxies (D. Thomas et al. 2008, in preparation) in order to investigate possible systematic differences between the disk and bulge components of S0 galaxies. The photometric and kinematic data of the combined data set allowed the construction of dynamical models of the objects to study the properties of the dark matter halos of flattened and rotating E and S0 galaxies (Thomas et al. 2005, 2007). In fact, the implementation of Schwarzschild's orbit superposition technique for axisymmetric potentials by Thomas et al. (2004) was used to derive the stellar mass-to-light ratios and dark matter halo parameters for a subsample of 17 galaxies. About 10%–50% of the mass inside the effective radius is dark with a central density that is at least 1 order of magnitude lower than the luminous mass density. The orbital system of the stars is reasonably close to isotropy, but the distribution function shows a lot of fine structure. This study was complementary to the one presented by Gerhard et al. (2001) focusing on round and nonrotating ellipticals.

The *HST* photometry is described in § 2. The spectroscopic galaxy sample, relative observations, and data reduction are described in § 3. The measured stellar kinematics and line indices are given in § 4. Conclusions are drawn in § 5.

2. *HST* PHOTOMETRY

As part of *HST* proposal 10884 (PI: G. Wegner), the galaxies GMP 0756, GMP 1176, GMP 1990, and GMP2440 were observed with Wide Field Planetary Camera 2 (WFPC2) on board the *HST* on 2007 April 18–24. For each galaxy two 300 s exposures were taken with the filter F622W. All exposures were performed with the telescope guiding in fine lock, which typically gave an rms tracking error of 0.003″. The centers of the galaxies were positioned on the Planetary Camera (PC) chip in order to get the best possible spatial resolution. This consists of 800×800 pixels of 0.0455×0.0455 arcsec^2 each, yielding a field of view of about 36×36 arcsec^2.

In the following we limit our photometric analysis to the PC chip, since we match the nuclear surface brightness profiles to available radially extended ground-based photometry.

The images were reduced using the standard reduction pipeline maintained by the Space Telescope Science Institute. Reduction steps include bias subtraction, dark current subtraction, and flat-fielding and are described in detail in Holtzman et al. (1995).

The isophotal profiles of the galaxies were analyzed by fitting the isophotes with ellipses following the prescriptions by Bender & Möllenhoff (1987). Foreground stars, cosmic rays, bad pixels, etc., were masked before fitting. Moreover, the centers of ellipses were allowed to vary. As a first step, the sky background was measured at the outer edges of the chip. Its final value was determined through the matching of the ground-based photometry (see below). A prominent dust lane present at the center of GMP 2440 was masked before performing the isophote analysis. Nevertheless, deviations from axisymmetric isophotes are present at the level of 2%. A dust lane is also visible near the center of GMP 1990, causing the center coordinates to drift along the minor axis away from the dust lane and deviations from axisymmetric isophotes at the level of 2%. Since masking the region affected by dust does not eliminate the drift or change the surface photometry, we give in Figure 1 and Table 1 the results of the isophotal shape analysis obtained without masking the dusty regions. The surface photometry was calibrated in the R band by matching the profiles given by Jørgensen et al. (1995) for GMP 2440 and by Paper I for the other three objects. The matching of the surface brightness was performed between 5″ and 15″ by determining the zero point and sky value that minimize the square surface brightness flux differences. It gives rms of 0.01 mag for GMP 0756, 0.066 mag for GMP 1990, 0.08 mag for GMP 1176, and 0.038 mag for GMP 2440. The position angles match within 1° and ellipticities within less than 0.02. The radial profiles of the azimuthally averaged surface brightness, ellipticity, position angle, center coordinates and third, fourth, and sixth cosine (a_3, a_4, and a_6) and sine (b_3, b_4, and b_6) Fourier coefficients are presented in Figure 1 and Table 1.

GMP 1176 has extremely high ellipticity ($\leq$0.75) and diskiness a_4 exceeding 10%. In this case the isophote fit program of Bender & Möllenhoff (1987) delivers a nonzero a_2 coefficient and a satisfactory description of the isophotes requires orders as high as a_{12}. The corresponding coefficient profiles are shown in Figure 2 and listed in Table 2. GMP 0756 and GMP 1990 also have high ellipticity ($\leq$0.65) but only mild ($\leq$2%) diskiness. GMP 2440 is slightly disky. Overall, the high ellipticities and the morphology of the dust distribution indicate that all four objects are very nearly edge-on.

3. SPECTROSCOPY

3.1. *Galaxy Sample*

All the observed galaxies (Table 3) belong to the sample of 35 E and S0 galaxies of the Coma Cluster studied in Paper I. For details about their morphological classification and relevant photometric properties (i.e., total magnitude, effective radius, mean surface brightness within effective radius, ellipticity at effective radius, and luminosity weighted a_4 parameter) the reader is referred to that paper.

3.2. *Long-Slit Spectroscopy*

Long-slit spectroscopic data of the sample galaxies were obtained with the 9.2 m Hobby-Eberly Telescope (HET) at McDonald Observatory, Texas, in queuing mode (Shetrone et al. 2007) and with the 2.4 m Hiltner telescope of the MDM Observatory at Kitt Peak, Arizona, in visitor mode during different runs between 2002 and 2005. Details of the instrumental setup of the observations carried out on 2002 February 26 to July 10 (run 1), 2003 April 11–15 (run 2), 2004 May 25–30 (run 3), 2005 May 10 (run 4), and 2005 April 7–10 (run 5) are given in Table 4.

Minor-axis spectra were obtained for all the sample galaxies, except for GMP 5975, which was observed only along a diagonal axis. The elliptical galaxies GMP 0144, GMP 2440, and GMP 4928 were observed along a diagonal axis too. Offset spectra with the slit parallel to the major axis were obtained only for the lenticular galaxies GMP 2417, GMP 3414, and GMP 5568. To perform a consistency check between measurements of stellar kinematics and line strength indices of different observing runs, diagonal-axis spectra of GMP 4928 were obtained in both runs 2 and 3 and minor-axis spectra of GMP 5568 were taken in both runs 2 and 5. In addition, spectra along the minor axis of GMP 0144 were taken to be compared with measurements of Paper II. The typical

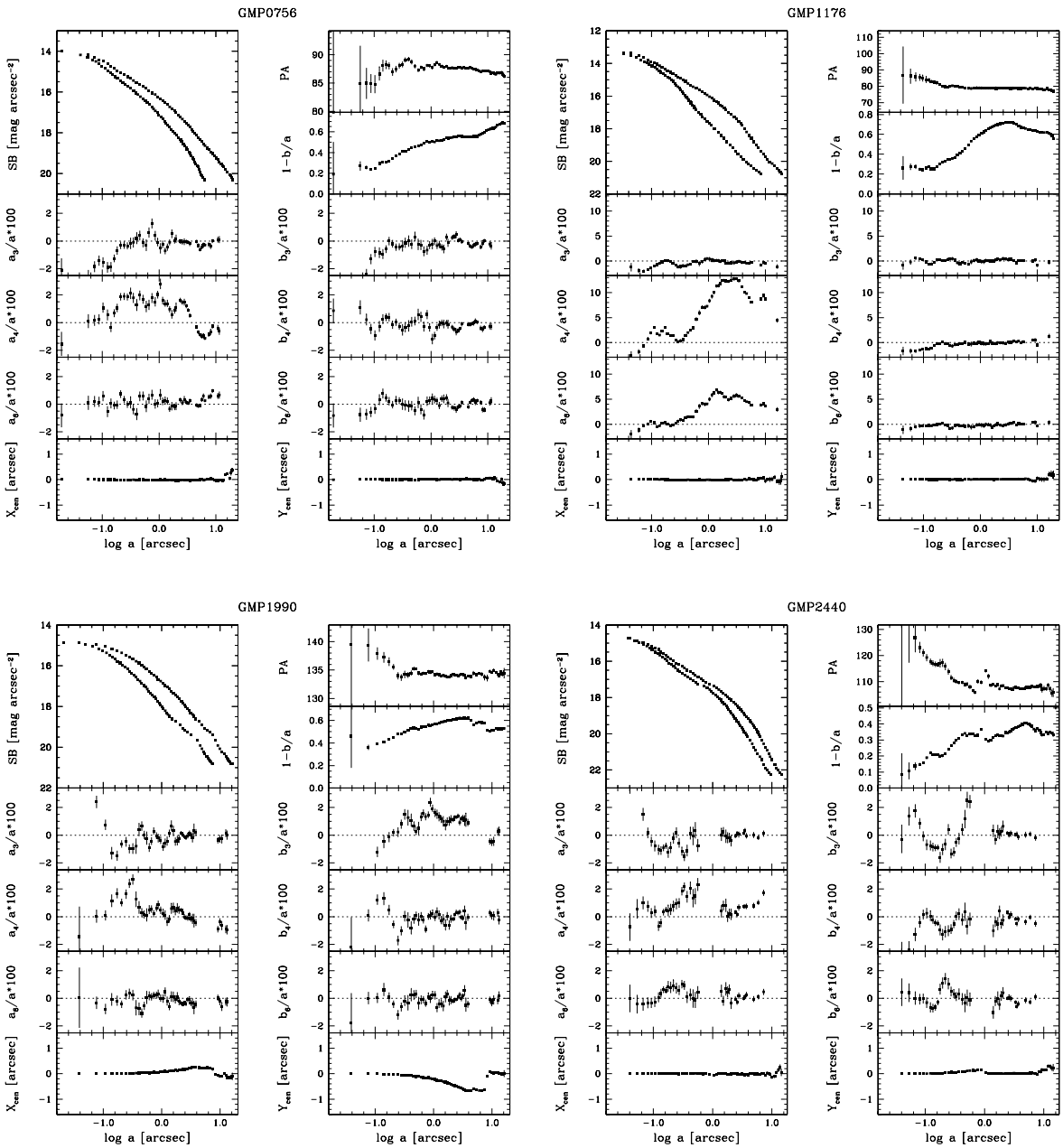

FIG. 1.— Isophotal parameters of the four galaxies recently observed with *HST* WFPC2 as a function of the logarithm of the semimajor axis distance in arcseconds. The radial profiles of *R*-band surface brightness, third, fourth, and sixth cosine Fourier coefficients (a_3, a_4, and a_6), and *x*-coordinate of the center (X_{cen}) are plotted in the left panels (*from top to bottom*). The surface brightness is shown along the major (*upper profile*) and minor (*lower profile*) axes. The radial profiles of position angle (P.A.), ellipticity ($1 - b/a$), third, fourth, and sixth sine Fourier coefficients (b_3, b_4, and b_6), and *y*-coordinate of the center (Y_{cen}) are plotted in the right panels (*from top to bottom*).

integration time of galaxy spectra was 3600 s. Total integration times and slit position angle of the galaxy spectra as well as the log of the spectroscopic observations are given in Table 3. At the beginning of each exposure the galaxy was centered on the slit either using acquisition images with HET or the guiding camera with the 2.4 m Hiltner telescope, which looks onto the slit.

In each run several spectra of giant stars with spectral type ranging from late-G to early-K were obtained to be used as templates in measuring stellar kinematics and line strength indices. The template stars were selected from Faber et al. (1985) and González (1993). In addition, we observed at least one flux standard star per night to calibrate the flux of the spectra before line indices were measured. Spectra of the comparison arc lamp were taken before and/or after object exposures (MDM) or at the end of the night (HET) to allow an accurate wavelength calibration.

All the spectra were bias-subtracted, flat-field corrected, cleaned of cosmic rays, corrected for bad columns, and wavelength-calibrated using standard IRAF[3] routines. The flat-field correction was performed by means of quartz lamp spectra in runs 1 and 4 and by means of both quartz lamp and twilight sky spectra in runs 2, 3, and 5. They were normalized and divided into all the spectra to correct for pixel-to-pixel sensitivity variations and large-scale illumination patterns due to slit vignetting. Cosmic rays were identified and corrected by interpolating over, as in Bender et al. (1994). The residual cosmic rays were corrected by manually editing the spectra. Each spectrum was rebinned using the wavelength solution obtained from the corresponding

[3] IRAF is distributed by NOAO, which is operated by AURA, Inc., under contract with the National Science Foundation.

TABLE 1

PHOTOMETRIC PARAMETERS OF THE SAMPLE GALAXIES OBSERVED WITH *HST* WFPC2

a (arcsec)	μ_R (mag arcsec^{-2})	e	P.A. (deg)	Δx_c (arcsec)	Δy_c (arcsec)	Err.[a] (arcsec)	a_3/a (×100)	b_3/a (×100)	a_4/a (×100)	b_4/a (×100)	a_6/a (×100)	b_6/a (×100)	Err.[b]
GMP 0756													
0.019 ± 0.005.....	14.013 ± 0.008	0.190 ± 0.312	79.8 ± 58.1	−0.001	−0.005	0.004	−2.11	−7.78	−1.54	0.87	−0.81	−0.82	0.87
0.057 ± 0.003.....	14.182 ± 0.015	0.271 ± 0.046	85.0 ± 6.6	0.000	0.000	0.002	−2.59	−4.66	0.11	1.10	0.10	−0.76	0.51
0.073 ± 0.001.....	14.306 ± 0.015	0.256 ± 0.018	84.9 ± 2.7	−0.001	0.000	0.001	−1.85	−2.42	0.15	0.20	0.19	−0.73	0.40
0.088 ± 0.001.....	14.418 ± 0.012	0.240 ± 0.011	84.9 ± 1.7	−0.002	−0.000	0.001	−1.42	−1.31	0.23	−0.46	0.17	−0.56	0.37
0.103 ± 0.001.....	14.504 ± 0.015	0.250 ± 0.010	84.8 ± 1.6	−0.003	−0.001	0.001	−1.54	−0.78	1.08	−0.93	0.59	−0.34	0.37
0.124 ± 0.001.....	14.608 ± 0.012	0.297 ± 0.009	86.7 ± 1.2	−0.003	−0.002	0.001	−1.90	−0.84	0.56	−0.28	−0.54	0.32	0.39
0.143 ± 0.001.....	14.729 ± 0.013	0.304 ± 0.008	88.1 ± 1.1	−0.003	−0.003	0.001	−1.87	−0.94	−0.33	0.24	0.05	0.78	0.36
0.162 ± 0.001.....	14.839 ± 0.014	0.305 ± 0.006	88.2 ± 0.8	−0.003	−0.003	0.001	−1.26	−0.59	0.68	0.38	−0.10	0.46	0.28
0.183 ± 0.001.....	14.947 ± 0.009	0.314 ± 0.005	88.0 ± 0.6	−0.005	−0.003	0.001	−0.69	0.00	1.06	0.39	−0.04	0.21	0.31
0.211 ± 0.001.....	15.034 ± 0.013	0.346 ± 0.005	87.0 ± 0.7	−0.005	−0.003	0.001	−0.32	−0.20	1.87	−0.18	0.73	−0.04	0.27
0.244 ± 0.001.....	15.134 ± 0.014	0.371 ± 0.005	87.5 ± 0.6	−0.005	−0.002	0.001	−0.29	−0.44	1.89	0.03	0.34	0.29	0.26
0.277 ± 0.001.....	15.236 ± 0.007	0.388 ± 0.004	88.1 ± 0.5	−0.005	−0.003	0.001	−0.35	−0.42	1.85	−0.26	−0.02	0.25	0.25
0.315 ± 0.002.....	15.338 ± 0.006	0.409 ± 0.004	88.3 ± 0.5	−0.006	−0.002	0.001	−0.17	−0.35	2.12	−0.53	0.12	0.01	0.41
0.354 ± 0.002.....	15.435 ± 0.006	0.415 ± 0.004	89.1 ± 0.5	−0.007	−0.001	0.001	−0.10	−0.12	1.79	−0.33	−0.37	−0.08	0.37
0.404 ± 0.002.....	15.525 ± 0.005	0.431 ± 0.003	89.2 ± 0.4	−0.004	−0.003	0.001	0.22	0.00	1.27	−0.24	−0.72	−0.15	0.41
0.459 ± 0.002.....	15.623 ± 0.004	0.445 ± 0.004	88.7 ± 0.4	−0.003	−0.004	0.002	0.39	−0.24	1.97	0.05	0.57	−0.11	0.35
0.522 ± 0.002.....	15.726 ± 0.004	0.458 ± 0.003	88.0 ± 0.4	−0.004	−0.006	0.002	−0.13	0.31	1.69	0.11	0.60	−0.49	0.32
0.593 ± 0.002.....	15.827 ± 0.004	0.468 ± 0.003	87.3 ± 0.3	−0.009	−0.003	0.002	−0.30	−0.24	1.16	0.59	−0.15	0.13	0.42
0.667 ± 0.002.....	15.930 ± 0.004	0.474 ± 0.003	87.8 ± 0.3	−0.010	−0.000	0.002	0.61	−0.28	1.28	0.42	0.39	−0.37	0.37
0.752 ± 0.003.....	16.028 ± 0.004	0.487 ± 0.003	87.5 ± 0.4	−0.017	0.005	0.002	1.26	−0.75	1.77	−0.29	0.68	−0.76	0.36
0.855 ± 0.003.....	16.124 ± 0.004	0.506 ± 0.003	88.1 ± 0.3	−0.010	0.000	0.002	0.39	−0.66	1.50	0.58	0.02	0.22	0.34
0.943 ± 0.003.....	16.226 ± 0.004	0.502 ± 0.002	88.0 ± 0.3	−0.006	0.001	0.002	−0.10	−0.29	2.02	−0.37	0.05	0.27	0.29
1.056 ± 0.005.....	16.324 ± 0.004	0.507 ± 0.003	87.7 ± 0.4	−0.013	0.001	0.003	−0.53	−0.23	2.81	−1.19	0.68	0.41	0.38
1.154 ± 0.004.....	16.423 ± 0.003	0.502 ± 0.002	88.2 ± 0.3	−0.019	0.004	0.003	−0.24	−0.01	1.59	−0.95	0.21	0.33	0.28
1.283 ± 0.004.....	16.521 ± 0.004	0.515 ± 0.002	88.6 ± 0.2	−0.003	−0.003	0.003	−0.72	−0.34	1.38	−0.35	0.26	0.23	0.24
1.406 ± 0.004.....	16.623 ± 0.004	0.515 ± 0.002	88.3 ± 0.2	−0.008	−0.003	0.003	−0.44	−0.26	1.39	−0.17	0.22	−0.10	0.26
1.539 ± 0.004.....	16.725 ± 0.003	0.520 ± 0.002	88.0 ± 0.2	−0.015	0.003	0.003	−0.10	−0.46	0.96	−0.02	−0.34	0.40	0.22
1.680 ± 0.005.....	16.822 ± 0.003	0.523 ± 0.002	87.8 ± 0.2	−0.024	0.010	0.004	0.52	−0.58	0.60	−0.10	−0.14	0.39	0.31
1.868 ± 0.005.....	16.924 ± 0.003	0.540 ± 0.002	88.0 ± 0.2	−0.010	−0.000	0.004	0.04	0.29	0.87	−0.03	−0.19	0.49	0.23
1.997 ± 0.006.....	17.021 ± 0.002	0.535 ± 0.002	87.7 ± 0.2	−0.023	0.010	0.004	0.16	−0.14	1.10	−0.14	−0.15	0.08	0.29
2.180 ± 0.005.....	17.123 ± 0.002	0.543 ± 0.001	87.7 ± 0.2	−0.034	0.004	0.004	...	...	...	...	...	...	...
2.372 ± 0.005.....	17.229 ± 0.002	0.545 ± 0.001	87.7 ± 0.2	−0.020	0.005	0.004	−0.03	0.25	1.62	−0.32	0.30	−0.23	0.17
2.571 ± 0.005.....	17.327 ± 0.003	0.550 ± 0.001	87.7 ± 0.2	−0.018	0.008	0.004	−0.08	0.32	1.47	−0.49	0.11	−0.29	0.17
2.781 ± 0.008.....	17.422 ± 0.003	0.553 ± 0.002	87.6 ± 0.2	−0.019	0.009	0.005	−0.05	0.46	1.48	−0.67	0.34	−0.38	0.25
3.003 ± 0.006.....	17.522 ± 0.003	0.557 ± 0.001	87.8 ± 0.1	−0.014	0.007	0.004	−0.06	0.05	1.19	−0.57	0.14	−0.19	0.16
3.224 ± 0.005.....	17.626 ± 0.003	0.558 ± 0.001	87.8 ± 0.1	−0.019	0.006	0.003	−0.08	0.12	0.91	−0.44	0.08	−0.16	0.14
3.467 ± 0.006.....	17.728 ± 0.002	0.559 ± 0.001	87.7 ± 0.1	−0.031	0.009	0.004	−0.20	−0.05	0.52	−0.11	0.23	0.11	0.16
3.714 ± 0.006.....	17.826 ± 0.002	0.556 ± 0.001	87.7 ± 0.1	−0.028	0.011	0.004	...	...	...	...	...	...	...
3.977 ± 0.006.....	17.929 ± 0.002	0.553 ± 0.001	87.7 ± 0.1	−0.026	0.013	0.004	...	...	...	...	...	...	...
4.278 ± 0.006.....	18.031 ± 0.002	0.553 ± 0.001	87.6 ± 0.1	−0.028	0.017	0.004	...	...	...	...	...	...	...
4.575 ± 0.006.....	18.131 ± 0.002	0.550 ± 0.001	87.7 ± 0.1	−0.025	0.012	0.004	−0.03	−0.18	−0.32	−0.13	−0.07	−0.21	0.14
4.908 ± 0.008.....	18.232 ± 0.002	0.551 ± 0.001	87.8 ± 0.1	−0.030	0.011	0.005	−0.32	−0.37	−0.71	−0.12	−0.12	0.13	0.15
5.235 ± 0.009.....	18.333 ± 0.002	0.551 ± 0.001	87.7 ± 0.1	−0.014	0.008	0.006	−0.62	−0.44	−0.88	−0.07	−0.08	0.28	0.12
5.598 ± 0.011.....	18.432 ± 0.002	0.554 ± 0.001	87.4 ± 0.1	0.002	−0.004	0.007	−0.42	−0.31	−0.97	−0.04	0.33	0.32	0.18
6.017 ± 0.011.....	18.531 ± 0.002	0.559 ± 0.001	87.5 ± 0.1	−0.006	−0.010	0.008	−0.30	−0.24	−0.98	0.12	0.59	0.12	0.18
6.423 ± 0.010.....	18.634 ± 0.003	0.559 ± 0.001	87.4 ± 0.1	−0.005	−0.003	0.007	−0.29	−0.17	−1.14	0.03	0.26	0.26	0.12
6.914 ± 0.013.....	18.735 ± 0.003	0.566 ± 0.001	87.1 ± 0.1	0.022	0.003	0.009	...	...	...	...	...	...	...
7.434 ± 0.013.....	18.834 ± 0.003	0.576 ± 0.001	87.0 ± 0.1	0.034	−0.017	0.009	−0.26	−0.42	−0.86	−0.40	0.53	0.12	0.17
8.029 ± 0.015.....	18.931 ± 0.004	0.585 ± 0.001	87.1 ± 0.1	0.017	−0.012	0.011	−0.37	−0.16	−0.70	−0.48	0.57	−0.39	0.20
8.634 ± 0.014.....	19.027 ± 0.004	0.594 ± 0.001	87.1 ± 0.1	0.003	0.009	0.010	−0.01	0.01	−0.28	−0.33	0.96	−0.42	0.14
9.429 ± 0.019.....	19.128 ± 0.005	0.611 ± 0.001	87.1 ± 0.1	−0.029	0.037	0.013	...	...	...	...	...	...	...
10.172 ± 0.023.....	19.220 ± 0.013	0.619 ± 0.001	87.1 ± 0.2	−0.051	0.062	0.016	...	...	...	...	...	...	...
10.837 ± 0.020.....	19.322 ± 0.013	0.624 ± 0.001	87.0 ± 0.1	−0.067	0.062	0.014	0.11	−0.22	−0.38	−0.27	0.59	0.11	0.22
11.480 ± 0.027.....	19.434 ± 0.005	0.627 ± 0.001	86.8 ± 0.2	−0.025	0.040	0.019	0.10	−0.36	−0.63	−0.27	0.66	0.24	0.26
12.235 ± 0.026.....	19.527 ± 0.006	0.636 ± 0.001	86.8 ± 0.1	−0.005	0.036	0.018	...	...	...	...	...	...	...
12.981 ± 0.029.....	19.610 ± 0.008	0.639 ± 0.001	86.7 ± 0.1	−0.065	0.077	0.021	...	...	...	...	...	...	...
13.797 ± 0.041.....	19.675 ± 0.027	0.647 ± 0.001	86.5 ± 0.2	−0.018	0.044	0.029	...	...	...	...	...	...	...
14.785 ± 0.066.....	19.776 ± 0.027	0.660 ± 0.002	86.8 ± 0.3	0.185	−0.043	0.047	...	...	...	...	...	...	...
15.917 ± 0.068.....	19.922 ± 0.007	0.671 ± 0.002	86.8 ± 0.3	0.225	−0.102	0.048	...	...	...	...	...	...	...
17.285 ± 0.094.....	20.059 ± 0.006	0.684 ± 0.002	86.8 ± 0.3	0.042	0.012	0.067	...	...	...	...	...	...	...
18.325 ± 0.123.....	20.117 ± 0.012	0.688 ± 0.003	86.6 ± 0.4	0.243	−0.128	0.087	...	...	...	...	...	...	...
19.010 ± 0.121.....	20.174 ± 0.015	0.686 ± 0.003	86.4 ± 0.4	0.354	−0.169	0.085	...	...	...	...	...	...	...
19.371 ± 0.116.....	20.307 ± 0.015	0.681 ± 0.003	86.2 ± 0.4	0.354	−0.156	0.082	...	...	...	...	...	...	...

TABLE 1—*Continued*

a (arcsec)	μ_R (mag arcsec^{-2})	e	P.A. (deg)	Δx_c (arcsec)	Δy_c (arcsec)	Err.[a] (arcsec)	a_3/a (×100)	b_3/a (×100)	a_4/a (×100)	b_4/a (×100)	a_6/a (×100)	b_6/a (×100)	Err.[b]
GMP 1176													
0.015 ± 0.002	13.206 ± 0.008	0.324 ± 0.155	106.1 ± 20.2	0.008	−0.003	0.002	1.33	2.89	−0.72	2.63	−0.86	1.19	0.49
0.044 ± 0.005	13.364 ± 0.008	0.262 ± 0.118	86.9 ± 17.5	0.000	0.000	0.004	−1.25	−0.88	−2.55	−1.68	−2.02	−1.13	0.85
0.059 ± 0.002	13.497 ± 0.020	0.274 ± 0.032	86.2 ± 4.7	−0.000	0.001	0.001	−1.93	−0.21	−1.81	−1.66	−1.18	−0.92	0.51
0.073 ± 0.001	13.628 ± 0.023	0.271 ± 0.019	85.7 ± 2.8	−0.000	0.001	0.001	−2.02	0.57	−0.65	−1.71	−0.27	−0.52	0.34
0.086 ± 0.001	13.798 ± 0.013	0.250 ± 0.013	85.3 ± 2.0	−0.000	0.000	0.001	−1.67	0.47	0.73	−1.47	0.07	−0.43	0.27
0.097 ± 0.001	13.902 ± 0.008	0.240 ± 0.012	84.9 ± 1.9	−0.000	−0.000	0.001	−1.44	0.29	1.89	−1.30	0.52	−0.40	0.23
0.111 ± 0.001	13.951 ± 0.010	0.260 ± 0.013	83.9 ± 1.9	−0.001	−0.001	0.001	−0.96	−0.26	3.09	−1.24	0.26	−0.36	0.20
0.126 ± 0.001	14.048 ± 0.016	0.277 ± 0.008	83.8 ± 1.2	−0.002	−0.001	0.001	−0.76	−0.69	1.86	−1.28	−0.48	−0.29	0.16
0.139 ± 0.001	14.141 ± 0.016	0.253 ± 0.007	83.1 ± 1.0	−0.002	−0.002	0.001	−0.46	−0.58	1.51	−1.03	−0.33	−0.33	0.17
0.154 ± 0.001	14.239 ± 0.012	0.252 ± 0.007	82.6 ± 1.1	−0.002	−0.002	0.001	−0.21	−0.18	2.30	−0.64	0.19	−0.23	0.14
0.171 ± 0.001	14.351 ± 0.010	0.270 ± 0.008	82.2 ± 1.2	−0.003	−0.002	0.001	0.02	0.26	2.99	−0.23	0.34	0.01	0.14
0.193 ± 0.001	14.442 ± 0.010	0.304 ± 0.005	81.4 ± 0.7	−0.004	−0.001	0.001	0.00	0.24	1.80	−0.23	0.02	0.08	0.14
0.215 ± 0.001	14.538 ± 0.009	0.318 ± 0.004	79.8 ± 0.5	−0.005	−0.001	0.001	−0.14	0.16	1.47	0.23	−0.30	0.22	0.16
0.239 ± 0.001	14.633 ± 0.008	0.334 ± 0.004	79.5 ± 0.5	−0.005	−0.001	0.001	−0.49	0.17	1.43	−0.19	−0.08	−0.17	0.17
0.266 ± 0.001	14.740 ± 0.008	0.348 ± 0.004	79.5 ± 0.5	−0.006	−0.001	0.001	−0.87	0.33	0.57	−0.24	0.18	−0.29	0.21
0.293 ± 0.002	14.830 ± 0.010	0.352 ± 0.005	80.1 ± 0.6	−0.007	−0.001	0.001	−1.16	0.46	0.19	−0.54	0.63	−0.84	0.32
0.322 ± 0.002	14.931 ± 0.009	0.357 ± 0.005	80.3 ± 0.6	−0.008	−0.001	0.001	−1.15	0.45	0.38	−0.68	0.86	−0.78	0.35
0.354 ± 0.001	15.032 ± 0.009	0.369 ± 0.004	80.2 ± 0.5	−0.009	−0.000	0.001	−0.99	0.24	0.59	−0.45	0.79	−0.27	0.28
0.395 ± 0.002	15.116 ± 0.009	0.393 ± 0.004	80.0 ± 0.5	−0.007	−0.001	0.001	−0.95	−0.36	1.47	−0.32	1.37	−0.17	0.25
0.436 ± 0.002	15.233 ± 0.006	0.412 ± 0.004	79.6 ± 0.5	−0.005	−0.002	0.001	−0.76	−0.61	2.02	−0.28	1.50	−0.27	0.18
0.481 ± 0.002	15.337 ± 0.007	0.432 ± 0.004	79.2 ± 0.5	−0.005	−0.003	0.002	−0.59	−0.30	2.46	−0.14	1.41	−0.27	0.20
0.534 ± 0.003	15.434 ± 0.006	0.454 ± 0.004	78.9 ± 0.5	−0.007	0.001	0.002	−0.13	−0.40	2.98	−0.01	1.40	−0.34	0.21
0.608 ± 0.005	15.536 ± 0.006	0.492 ± 0.006	78.6 ± 0.7	−0.008	0.004	0.003	−0.04	−0.60	4.70	−0.25	2.63	−0.42	0.33
0.692 ± 0.007	15.635 ± 0.007	0.530 ± 0.007	78.7 ± 0.8	−0.004	0.000	0.005	−0.54	−0.16	6.00	−0.27	3.56	−0.58	0.48
0.779 ± 0.009	15.735 ± 0.007	0.558 ± 0.007	78.9 ± 0.8	−0.005	0.000	0.006	−0.13	0.12	7.09	−0.10	4.11	−0.46	0.36
0.866 ± 0.009	15.836 ± 0.008	0.578 ± 0.006	78.9 ± 0.7	−0.009	0.005	0.006	0.38	0.23	7.07	−0.11	3.99	−0.12	0.38
0.946 ± 0.010	15.934 ± 0.009	0.591 ± 0.006	79.0 ± 0.7	−0.012	0.008	0.007	0.49	0.04	7.28	0.05	4.06	−0.05	0.26
1.046 ± 0.012	16.041 ± 0.009	0.611 ± 0.006	79.0 ± 0.8	−0.014	0.010	0.009	0.42	−0.12	8.36	−0.10	5.01	−0.22	0.38
1.148 ± 0.014	16.149 ± 0.009	0.628 ± 0.007	78.9 ± 0.8	−0.010	0.006	0.010	0.19	−0.15	9.24	−0.19	5.82	−0.25	0.44
1.246 ± 0.016	16.243 ± 0.010	0.638 ± 0.007	78.8 ± 0.8	−0.010	0.004	0.011	0.10	0.12	10.02	−0.26	6.27	−0.04	0.35
1.375 ± 0.019	16.338 ± 0.010	0.656 ± 0.007	78.8 ± 0.9	−0.007	0.004	0.014	0.15	0.08	11.30	−0.15	6.85	−0.09	0.30
1.489 ± 0.020	16.441 ± 0.011	0.666 ± 0.006	78.9 ± 0.8	−0.007	0.005	0.014	0.08	0.04	11.39	0.20	6.33	−0.16	0.35
1.604 ± 0.022	16.538 ± 0.011	0.672 ± 0.006	78.9 ± 0.8	−0.004	0.005	0.015	−0.10	0.09	11.77	−0.15	6.40	−0.54	0.30
1.741 ± 0.025	16.626 ± 0.011	0.683 ± 0.006	78.9 ± 0.9	−0.006	0.008	0.018	0.06	0.09	12.38	−0.11	6.15	−0.26	0.25
1.874 ± 0.026	16.718 ± 0.011	0.691 ± 0.006	78.9 ± 0.8	−0.007	0.010	0.019	0.03	0.24	12.43	−0.18	5.48	−0.10	0.26
2.005 ± 0.028	16.819 ± 0.010	0.695 ± 0.006	78.8 ± 0.8	−0.004	0.002	0.020	−0.43	0.41	12.31	0.00	5.39	0.06	0.26
2.254 ± 0.030	16.978 ± 0.007	0.705 ± 0.006	78.9 ± 0.8	−0.003	0.008	0.021	−0.39	0.23	12.25	−0.02	4.83	−0.21	0.30
2.526 ± 0.034	17.132 ± 0.007	0.715 ± 0.005	78.9 ± 0.8	−0.001	0.010	0.024	−0.41	0.50	12.49	−0.06	5.18	−0.27	0.34
2.803 ± 0.038	17.271 ± 0.006	0.719 ± 0.005	78.8 ± 0.8	−0.005	0.011	0.027	−0.36	0.41	12.74	−0.11	5.59	−0.10	0.36
3.091 ± 0.042	17.403 ± 0.006	0.721 ± 0.005	78.8 ± 0.8	−0.007	0.012	0.030	−0.17	0.38	12.79	0.07	5.75	0.08	0.32
3.391 ± 0.045	17.541 ± 0.006	0.721 ± 0.005	78.7 ± 0.8	−0.005	0.014	0.032	−0.05	0.44	12.34	0.09	5.59	0.14	0.28
3.684 ± 0.051	17.687 ± 0.005	0.716 ± 0.005	78.7 ± 0.8	−0.005	0.015	0.036	...	...	...	...	...	...	...
3.889 ± 0.050	17.789 ± 0.005	0.712 ± 0.005	78.7 ± 0.7	−0.004	0.016	0.035	−0.33	0.06	11.13	0.36	5.21	0.32	0.22
4.306 ± 0.050	17.991 ± 0.004	0.706 ± 0.005	78.8 ± 0.7	0.000	0.006	0.036	−0.23	−0.36	10.11	0.06	4.76	−0.15	0.20
4.676 ± 0.056	18.195 ± 0.004	0.683 ± 0.005	78.7 ± 0.7	−0.005	0.023	0.039	−0.45	0.07	9.80	0.30	4.49	0.11	0.15
5.157 ± 0.053	18.392 ± 0.003	0.675 ± 0.005	78.7 ± 0.6	0.016	0.005	0.038	−0.38	0.06	9.07	0.01	4.46	0.04	0.18
5.661 ± 0.052	18.589 ± 0.003	0.667 ± 0.004	78.8 ± 0.6	0.009	0.015	0.036	−0.23	0.04	8.08	0.22	3.76	−0.01	0.18
6.190 ± 0.060	18.786 ± 0.003	0.659 ± 0.005	78.8 ± 0.6	−0.003	0.031	0.043	...	...	...	...	...	...	...
6.797 ± 0.072	18.978 ± 0.003	0.647 ± 0.005	78.4 ± 0.7	−0.006	0.006	0.051	...	...	...	...	...	...	...
7.536 ± 0.079	19.165 ± 0.003	0.647 ± 0.005	78.6 ± 0.7	0.025	−0.013	0.056	...	...	...	...	...	...	...
8.281 ± 0.086	19.352 ± 0.003	0.642 ± 0.005	78.5 ± 0.7	0.050	−0.048	0.061	−0.72	−0.06	8.74	0.55	3.92	0.39	0.25
9.114 ± 0.101	19.526 ± 0.004	0.639 ± 0.006	78.7 ± 0.7	0.055	−0.057	0.072	−0.30	0.22	9.39	0.56	4.08	0.40	0.37
10.019 ± 0.101	19.691 ± 0.006	0.632 ± 0.005	78.7 ± 0.6	−0.061	0.045	0.071	−0.43	−0.90	8.69	−0.45	3.65	−0.30	0.30
10.898 ± 0.099	19.861 ± 0.006	0.624 ± 0.005	78.4 ± 0.6	−0.001	0.006	0.070	...	...	...	...	...	...	...
11.918 ± 0.125	20.029 ± 0.009	0.618 ± 0.006	78.2 ± 0.7	0.002	0.000	0.089	...	...	...	...	...	...	...
13.164 ± 0.132	20.137 ± 0.021	0.618 ± 0.005	77.9 ± 0.7	0.016	0.002	0.094	...	...	...	...	...	...	...
14.672 ± 0.115	20.288 ± 0.021	0.620 ± 0.004	78.4 ± 0.5	0.093	0.031	0.081	...	...	...	...	...	...	...
16.144 ± 0.119	20.444 ± 0.016	0.611 ± 0.004	77.8 ± 0.5	−0.061	0.197	0.084	−1.08	−0.22	4.44	1.31	2.97	0.32	0.45
17.500 ± 0.173	20.536 ± 0.019	0.606 ± 0.005	77.9 ± 0.7	−0.085	0.234	0.123	...	...	...	...	...	...	...
18.545 ± 0.191	20.648 ± 0.021	0.588 ± 0.006	77.4 ± 0.7	−0.058	0.173	0.135	...	...	...	...	...	...	...
19.222 ± 0.233	20.756 ± 0.021	0.562 ± 0.007	77.2 ± 0.9	0.111	0.193	0.165	...	...	...	...	...	...	...

TABLE 1—*Continued*

a (arcsec)	μ_R (mag arcsec^{-2})	e	P.A. (deg)	Δx_c (arcsec)	Δy_c (arcsec)	Err.[a] (arcsec)	a_3/a (×100)	b_3/a (×100)	a_4/a (×100)	b_4/a (×100)	a_6/a (×100)	b_6/a (×100)	Err.[b]
					GMP 1990								
0.015 ± 0.000.....	14.771 ± 0.010	0.000 ± 0.000	113.7 ± 0.0	0.016	0.021	0.000	0.00	0.00	0.00	0.00	0.00	0.00	0.00
0.039 ± 0.014.....	14.853 ± 0.016	0.458 ± 0.278	139.6 ± 32.0	0.000	0.000	0.010	5.57	−6.90	−1.45	−2.22	0.05	−1.80	2.18
0.077 ± 0.002.....	14.967 ± 0.012	0.361 ± 0.023	139.4 ± 2.9	0.000	−0.004	0.001	2.41	−3.67	0.01	0.10	−0.32	0.02	0.45
0.109 ± 0.001.....	15.062 ± 0.009	0.393 ± 0.009	137.9 ± 1.1	0.003	−0.010	0.001	0.75	−1.21	0.09	1.24	−0.77	0.03	0.37
0.140 ± 0.001.....	15.158 ± 0.011	0.410 ± 0.008	137.2 ± 0.9	0.002	−0.017	0.001	−1.30	−0.47	1.15	1.31	−0.08	0.64	0.46
0.172 ± 0.001.....	15.265 ± 0.012	0.434 ± 0.006	136.5 ± 0.8	0.002	−0.025	0.001	−1.50	−0.15	1.69	0.49	−0.17	0.06	0.37
0.205 ± 0.001.....	15.370 ± 0.011	0.450 ± 0.004	135.6 ± 0.5	0.005	−0.032	0.001	−0.63	0.17	1.03	−0.55	−0.43	−0.43	0.27
0.245 ± 0.002.....	15.473 ± 0.008	0.478 ± 0.005	134.0 ± 0.6	0.009	−0.041	0.001	−0.48	0.22	1.63	−1.72	0.25	−1.19	0.35
0.280 ± 0.002.....	15.574 ± 0.007	0.482 ± 0.005	133.7 ± 0.6	0.012	−0.050	0.001	−0.99	0.79	2.41	−1.02	0.37	−0.63	0.33
0.319 ± 0.002.....	15.680 ± 0.008	0.494 ± 0.005	134.2 ± 0.6	0.015	−0.058	0.002	−0.97	1.50	2.69	0.04	0.23	−0.18	0.37
0.365 ± 0.002.....	15.778 ± 0.008	0.516 ± 0.004	134.1 ± 0.5	0.019	−0.068	0.002	−0.80	1.26	1.27	−0.24	−0.68	−0.32	0.56
0.411 ± 0.002.....	15.872 ± 0.007	0.525 ± 0.003	134.5 ± 0.4	0.026	−0.078	0.002	0.37	1.07	0.68	−0.80	−0.76	0.26	0.46
0.458 ± 0.002.....	15.969 ± 0.006	0.531 ± 0.002	135.2 ± 0.3	0.028	−0.091	0.001	0.66	0.65	0.30	−0.15	−1.07	0.24	0.34
0.503 ± 0.001.....	16.070 ± 0.006	0.524 ± 0.002	135.2 ± 0.2	0.033	−0.104	0.001	0.02	0.30	0.17	0.07	−0.54	0.32	0.30
0.552 ± 0.002.....	16.169 ± 0.006	0.524 ± 0.003	134.4 ± 0.3	0.039	−0.117	0.002	−0.22	0.51	0.13	−0.19	0.07	−0.34	0.46
0.610 ± 0.002.....	16.267 ± 0.007	0.537 ± 0.002	134.3 ± 0.3	0.037	−0.131	0.002	−0.89	1.33	0.52	0.03	0.18	−0.11	0.32
0.668 ± 0.002.....	16.368 ± 0.007	0.542 ± 0.002	134.4 ± 0.3	0.043	−0.143	0.002	−0.43	1.60	0.55	−0.22	0.11	−0.11	0.27
0.731 ± 0.002.....	16.466 ± 0.004	0.542 ± 0.002	134.4 ± 0.2	0.056	−0.158	0.002	0.30	1.33	0.21	−0.89	0.21	−0.35	0.26
0.813 ± 0.003.....	16.567 ± 0.005	0.558 ± 0.002	134.8 ± 0.2	0.060	−0.173	0.002	−0.03	1.47	0.62	0.02	0.25	0.15	0.24
0.875 ± 0.004.....	16.665 ± 0.005	0.552 ± 0.003	134.7 ± 0.3	0.065	−0.191	0.002	−0.21	2.38	0.86	0.12	0.32	−0.01	0.31
0.961 ± 0.004.....	16.759 ± 0.004	0.558 ± 0.002	134.7 ± 0.3	0.072	−0.212	0.003	−0.37	1.93	0.47	0.21	0.02	0.23	0.27
1.057 ± 0.003.....	16.859 ± 0.004	0.568 ± 0.002	134.2 ± 0.2	0.080	−0.231	0.002	−0.83	1.61	0.24	−0.00	−0.02	0.21	0.30
1.147 ± 0.004.....	16.956 ± 0.004	0.572 ± 0.002	134.3 ± 0.2	0.085	−0.250	0.003	−0.57	1.51	0.12	0.35	0.46	−0.68	0.33
1.241 ± 0.004.....	17.052 ± 0.004	0.574 ± 0.002	134.2 ± 0.2	0.091	−0.272	0.003	−0.43	1.33	−0.34	0.13	−0.20	−0.38	0.33
1.359 ± 0.004.....	17.149 ± 0.004	0.582 ± 0.002	133.9 ± 0.2	0.105	−0.293	0.003	0.14	1.16	−0.16	−0.27	−0.59	−0.39	0.28
1.471 ± 0.005.....	17.247 ± 0.004	0.588 ± 0.002	134.1 ± 0.2	0.112	−0.313	0.004	0.69	1.00	0.58	−0.18	0.12	−0.55	0.38
1.592 ± 0.005.....	17.330 ± 0.008	0.594 ± 0.002	133.9 ± 0.2	0.118	−0.339	0.004	0.32	0.73	0.65	−0.59	0.11	0.10	0.37
1.714 ± 0.005.....	17.425 ± 0.008	0.598 ± 0.002	133.7 ± 0.2	0.136	−0.358	0.003	−0.46	0.99	0.40	0.03	−0.07	0.32	0.30
1.853 ± 0.006.....	17.531 ± 0.004	0.600 ± 0.002	133.9 ± 0.2	0.126	−0.393	0.004	−0.40	1.02	0.64	−0.60	0.10	−0.17	0.35
1.987 ± 0.006.....	17.629 ± 0.003	0.600 ± 0.002	133.9 ± 0.2	0.139	−0.420	0.004	−0.27	1.15	0.50	−0.15	−0.21	−0.13	0.29
2.157 ± 0.004.....	17.734 ± 0.003	0.610 ± 0.001	134.2 ± 0.1	0.157	−0.440	0.003	0.16	1.10	0.48	−0.17	−0.36	−0.20	0.14
2.295 ± 0.004.....	17.832 ± 0.003	0.606 ± 0.001	134.2 ± 0.1	0.164	−0.474	0.003	−0.01	1.32	0.27	0.17	−0.47	−0.08	0.12
2.445 ± 0.005.....	17.927 ± 0.003	0.610 ± 0.001	134.1 ± 0.1	0.172	−0.497	0.003	−0.09	1.30	0.00	0.33	−0.31	−0.09	0.13
2.609 ± 0.006.....	18.021 ± 0.003	0.613 ± 0.001	134.0 ± 0.2	0.179	−0.521	0.004	−0.18	1.39	−0.07	0.28	−0.38	0.08	0.17
2.810 ± 0.006.....	18.111 ± 0.003	0.623 ± 0.001	134.2 ± 0.1	0.178	−0.545	0.004	−0.06	0.90	−0.10	0.34	−0.09	0.27	0.18
2.990 ± 0.007.....	18.206 ± 0.003	0.615 ± 0.001	134.2 ± 0.2	0.207	−0.580	0.005	0.15	1.20	0.14	−0.04	−0.09	−0.02	0.19
3.166 ± 0.008.....	18.300 ± 0.003	0.616 ± 0.001	134.2 ± 0.2	0.215	−0.606	0.006	0.01	1.28	−0.16	−0.09	−0.35	0.18	0.19
3.389 ± 0.014.....	18.392 ± 0.003	0.623 ± 0.002	134.1 ± 0.3	0.247	−0.625	0.010	−0.16	1.05	−0.16	0.42	−0.36	0.57	0.37
3.587 ± 0.016.....	18.490 ± 0.005	0.618 ± 0.002	133.7 ± 0.3	0.253	−0.664	0.011	0.35	1.10	−0.28	−0.46	−0.67	−0.48	0.49
3.880 ± 0.011.....	18.589 ± 0.003	0.619 ± 0.001	134.0 ± 0.2	0.264	−0.666	0.008	0.20	0.92	−0.42	−0.04	−0.42	−0.43	0.25
4.321 ± 0.018.....	18.719 ± 0.003	0.598 ± 0.002	133.9 ± 0.3	0.232	−0.671	0.013	...	...	...	...	...	...	...
4.787 ± 0.026.....	18.889 ± 0.003	0.564 ± 0.003	134.4 ± 0.4	0.216	−0.593	0.018	...	...	...	...	...	...	...
5.383 ± 0.022.....	19.061 ± 0.004	0.574 ± 0.002	134.2 ± 0.3	0.238	−0.627	0.016	...	...	...	...	...	...	...
6.062 ± 0.021.....	19.157 ± 0.005	0.586 ± 0.002	134.4 ± 0.2	0.250	−0.668	0.015	...	...	...	...	...	...	...
6.704 ± 0.034.....	19.252 ± 0.005	0.581 ± 0.003	134.3 ± 0.4	0.233	−0.662	0.024	...	...	...	...	...	...	...
7.484 ± 0.057.....	19.403 ± 0.004	0.578 ± 0.005	133.7 ± 0.5	0.165	−0.626	0.040	...	...	...	...	...	...	...
8.343 ± 0.061.....	19.664 ± 0.004	0.509 ± 0.005	133.6 ± 0.6	−0.025	−0.109	0.043	...	...	...	...	...	...	...
9.176 ± 0.024.....	19.916 ± 0.006	0.500 ± 0.002	134.7 ± 0.2	−0.080	0.064	0.017	−0.38	−0.45	−0.90	0.28	0.05	−0.11	0.23
9.937 ± 0.028.....	20.074 ± 0.007	0.509 ± 0.002	134.6 ± 0.2	−0.098	0.038	0.020	−0.28	−0.50	−0.38	0.07	−0.24	−0.30	0.27
10.724 ± 0.040.....	20.201 ± 0.008	0.511 ± 0.003	135.0 ± 0.3	−0.089	0.033	0.028	−0.28	−0.45	−0.64	0.06	−0.59	−0.11	0.33
11.760 ± 0.034.....	20.321 ± 0.010	0.531 ± 0.002	134.6 ± 0.2	−0.004	0.054	0.024	...	...	...	...	...	...	...
12.515 ± 0.038.....	20.437 ± 0.013	0.526 ± 0.002	134.2 ± 0.2	−0.058	0.048	0.027	0.15	0.24	−0.91	0.28	−0.24	−0.15	0.28
13.158 ± 0.045.....	20.541 ± 0.014	0.525 ± 0.002	134.0 ± 0.3	−0.150	0.018	0.032	0.00	0.29	−0.94	−0.23	−0.26	0.17	0.33
13.724 ± 0.056.....	20.612 ± 0.019	0.524 ± 0.003	134.3 ± 0.3	−0.161	0.020	0.039	...	...	...	...	...	...	...
14.310 ± 0.056.....	20.666 ± 0.025	0.527 ± 0.003	134.7 ± 0.3	−0.147	0.014	0.039	...	...	...	...	...	...	...
14.843 ± 0.072.....	20.728 ± 0.030	0.526 ± 0.003	134.4 ± 0.4	−0.163	−0.027	0.051	...	...	...	...	...	...	...
15.322 ± 0.073.....	20.790 ± 0.041	0.525 ± 0.003	134.3 ± 0.4	−0.132	−0.017	0.051	...	...	...	...	...	...	...
15.669 ± 0.092.....	20.808 ± 0.055	0.525 ± 0.004	134.5 ± 0.5	−0.143	−0.012	0.065	...	...	...	...	...	...	...
16.136 ± 0.192.....	20.785 ± 0.055	0.528 ± 0.008	134.5 ± 0.9	−0.105	−0.003	0.136	...	...	...	...	...	...	...

TABLE 1—*Continued*

a (arcsec)	μ_R (mag arcsec^{-2})	e	P.A. (deg)	Δx_c (arcsec)	Δy_c (arcsec)	Err.[a] (arcsec)	a_3/a (×100)	b_3/a (×100)	a_4/a (×100)	b_4/a (×100)	a_6/a (×100)	b_6/a (×100)	Err.[b]
					GMP 2440								
0.015 ± 0.004.....	14.567 ± 0.008	0.109 ± 0.299	188.2 ± 88.3	0.000	0.005	0.002	−5.18	−3.32	1.84	3.00	−0.27	0.51	0.95
0.040 ± 0.004.....	14.725 ± 0.008	0.083 ± 0.135	139.8 ± 50.9	0.000	0.000	0.003	3.99	−0.30	−0.75	−2.82	−0.01	0.44	1.00
0.053 ± 0.002.....	14.860 ± 0.009	0.108 ± 0.053	132.9 ± 15.7	0.000	−0.000	0.002	3.88	1.38	0.55	−2.44	−0.41	0.41	0.67
0.067 ± 0.001.....	14.991 ± 0.022	0.136 ± 0.022	126.7 ± 5.3	0.000	0.000	0.001	1.50	1.76	1.00	−1.28	−0.43	0.02	0.47
0.080 ± 0.001.....	15.094 ± 0.021	0.148 ± 0.009	123.1 ± 2.2	0.000	0.002	0.000	0.16	0.84	0.75	−0.41	−0.33	−0.06	0.39
0.092 ± 0.001.....	15.167 ± 0.011	0.156 ± 0.006	121.0 ± 1.4	0.000	0.003	0.000	−0.48	−0.08	0.27	0.16	−0.34	−0.02	0.36
0.106 ± 0.001.....	15.257 ± 0.014	0.190 ± 0.007	119.2 ± 1.3	0.000	0.005	0.000	−0.78	−0.70	0.42	0.25	−0.25	−0.32	0.39
0.122 ± 0.001.....	15.364 ± 0.012	0.223 ± 0.007	117.7 ± 1.2	−0.000	0.007	0.001	−1.06	−0.75	−0.66	0.06	0.08	−0.65	0.36
0.135 ± 0.001.....	15.473 ± 0.012	0.211 ± 0.007	117.1 ± 1.1	−0.001	0.009	0.001	−1.11	−0.87	−0.45	−0.20	0.37	−0.71	0.31
0.149 ± 0.001.....	15.578 ± 0.011	0.209 ± 0.006	116.7 ± 1.0	−0.001	0.012	0.001	−0.91	−0.92	0.34	−0.43	0.63	−0.66	0.24
0.163 ± 0.001.....	15.673 ± 0.008	0.211 ± 0.005	116.6 ± 0.9	−0.001	0.015	0.001	−0.79	−0.89	0.52	−0.47	0.57	−0.31	0.20
0.178 ± 0.001.....	15.791 ± 0.010	0.197 ± 0.009	117.0 ± 1.6	0.000	0.020	0.001	−1.24	−1.61	0.44	−0.96	0.86	0.67	0.40
0.197 ± 0.002.....	15.890 ± 0.017	0.201 ± 0.009	117.2 ± 1.5	0.000	0.025	0.001	−0.88	−1.03	0.53	−1.30	0.80	1.11	0.41
0.218 ± 0.002.....	15.980 ± 0.016	0.216 ± 0.008	115.8 ± 1.4	0.001	0.030	0.001	−0.21	−0.67	0.76	−1.08	0.91	1.42	0.41
0.244 ± 0.002.....	16.096 ± 0.008	0.244 ± 0.007	113.9 ± 1.1	0.000	0.037	0.001	0.18	0.41	0.93	−1.01	0.74	1.04	0.39
0.273 ± 0.002.....	16.193 ± 0.010	0.268 ± 0.007	111.6 ± 1.0	−0.002	0.045	0.001	−0.56	−1.33	0.99	−0.89	0.59	0.50	0.35
0.303 ± 0.002.....	16.278 ± 0.009	0.284 ± 0.007	110.6 ± 1.0	−0.001	0.053	0.001	−1.18	−1.23	1.85	−0.53	1.03	0.32	0.30
0.335 ± 0.002.....	16.377 ± 0.007	0.297 ± 0.006	110.1 ± 0.8	0.001	0.061	0.001	−1.54	−0.53	2.15	0.05	0.94	0.13	0.32
0.371 ± 0.002.....	16.474 ± 0.006	0.312 ± 0.005	109.6 ± 0.6	0.000	0.068	0.001	−1.11	−0.25	1.44	0.19	0.08	0.30	0.42
0.420 ± 0.002.....	16.575 ± 0.006	0.334 ± 0.005	109.7 ± 0.6	0.000	0.080	0.002	0.13	0.40	2.05	−0.20	0.27	−0.05	0.43
0.467 ± 0.003.....	16.675 ± 0.006	0.341 ± 0.005	109.0 ± 0.7	0.004	0.091	0.002	−0.07	1.16	1.34	0.36	−0.02	−0.35	0.67
0.512 ± 0.003.....	16.773 ± 0.007	0.325 ± 0.006	109.1 ± 0.8	0.008	0.104	0.002	0.35	2.55	1.48	−0.69	−0.12	0.05	0.59
0.565 ± 0.004.....	16.870 ± 0.006	0.337 ± 0.006	108.0 ± 0.8	0.013	0.114	0.003	−0.74	2.42	2.33	−0.18	0.41	−0.08	0.47
0.637 ± 0.003.....	16.966 ± 0.005	0.338 ± 0.005	106.6 ± 0.6	0.011	0.124	0.002	...	...	...	...	...	...	...
0.694 ± 0.004.....	17.067 ± 0.005	0.325 ± 0.005	105.9 ± 0.7	0.007	0.132	0.002	...	...	...	...	...	...	...
0.774 ± 0.005.....	17.166 ± 0.005	0.329 ± 0.006	110.1 ± 0.8	0.000	0.140	0.004	...	...	...	...	...	...	...
0.880 ± 0.006.....	17.267 ± 0.005	0.366 ± 0.006	109.8 ± 0.7	−0.015	0.145	0.004	...	...	...	...	...	...	...
1.041 ± 0.004.....	17.372 ± 0.004	0.305 ± 0.004	114.1 ± 0.6	−0.047	0.043	0.003	...	...	...	...	...	...	...
1.164 ± 0.008.....	17.472 ± 0.004	0.292 ± 0.007	112.0 ± 0.9	−0.018	−0.000	0.005	...	...	...	...	...	...	...
1.272 ± 0.005.....	17.571 ± 0.003	0.297 ± 0.004	108.6 ± 0.6	0.000	0.001	0.004	...	...	...	...	...	...	...
1.404 ± 0.006.....	17.666 ± 0.003	0.319 ± 0.004	108.8 ± 0.5	−0.004	0.001	0.004	0.04	0.31	0.40	−1.02	0.54	−1.02	0.45
1.526 ± 0.005.....	17.760 ± 0.003	0.325 ± 0.003	108.2 ± 0.4	−0.010	0.001	0.004	0.23	−0.33	0.81	−0.39	−0.18	−0.20	0.36
1.670 ± 0.007.....	17.854 ± 0.004	0.332 ± 0.004	108.8 ± 0.5	−0.005	−0.008	0.005	−0.08	0.27	0.83	−0.50	0.69	0.01	0.48
1.790 ± 0.008.....	17.953 ± 0.004	0.328 ± 0.004	107.2 ± 0.6	−0.017	−0.002	0.006	−0.19	0.10	0.01	0.41	0.47	−0.46	0.40
1.917 ± 0.008.....	18.055 ± 0.003	0.326 ± 0.004	108.5 ± 0.5	−0.015	−0.006	0.006	−0.18	0.24	0.23	−0.50	0.65	0.19	0.36
2.060 ± 0.009.....	18.149 ± 0.006	0.325 ± 0.004	108.5 ± 0.5	−0.003	0.004	0.006	−0.40	0.63	0.18	−0.25	−0.36	0.39	0.42
2.263 ± 0.006.....	18.255 ± 0.006	0.344 ± 0.002	107.8 ± 0.3	0.006	0.004	0.004	...	...	...	...	...	...	...
2.419 ± 0.004.....	18.369 ± 0.003	0.343 ± 0.002	107.7 ± 0.2	−0.008	0.004	0.003	−0.08	0.16	0.35	0.29	−0.05	0.01	0.14
2.589 ± 0.005.....	18.469 ± 0.004	0.349 ± 0.002	107.4 ± 0.2	−0.022	0.005	0.004	0.11	0.02	0.16	−0.02	−0.28	0.06	0.16
2.755 ± 0.006.....	18.568 ± 0.004	0.354 ± 0.002	107.2 ± 0.2	−0.027	0.007	0.004	0.05	0.12	0.67	0.17	0.19	0.00	0.20
2.948 ± 0.008.....	18.671 ± 0.003	0.366 ± 0.002	106.9 ± 0.3	−0.017	0.008	0.006	...	...	...	...	...	...	...
3.151 ± 0.007.....	18.772 ± 0.003	0.373 ± 0.002	107.7 ± 0.2	−0.022	0.015	0.005	...	...	...	...	...	...	...
3.358 ± 0.006.....	18.871 ± 0.004	0.380 ± 0.001	107.9 ± 0.2	−0.014	0.012	0.004	0.14	0.04	0.74	−0.14	−0.01	−0.29	0.14
3.529 ± 0.007.....	18.971 ± 0.003	0.378 ± 0.002	107.7 ± 0.2	−0.032	0.009	0.005	0.35	0.09	0.74	−0.51	0.12	−0.58	0.19
3.731 ± 0.010.....	19.068 ± 0.004	0.382 ± 0.002	107.6 ± 0.3	−0.029	0.002	0.007	−0.04	−0.15	0.76	−0.19	0.26	−0.40	0.20
3.982 ± 0.011.....	19.168 ± 0.004	0.390 ± 0.002	107.2 ± 0.3	−0.031	0.003	0.008	...	...	...	...	...	...	...
4.237 ± 0.008.....	19.272 ± 0.003	0.397 ± 0.002	107.5 ± 0.2	0.014	0.007	0.006	...	...	...	...	...	...	...
4.454 ± 0.012.....	19.362 ± 0.006	0.397 ± 0.002	107.4 ± 0.3	0.004	0.014	0.009	...	...	...	...	...	...	...
4.702 ± 0.012.....	19.462 ± 0.006	0.403 ± 0.002	107.4 ± 0.2	0.002	0.023	0.008	...	...	...	...	...	...	...
4.955 ± 0.013.....	19.571 ± 0.005	0.408 ± 0.002	107.6 ± 0.3	0.022	0.001	0.009	0.01	0.03	0.80	−0.39	−0.05	−0.14	0.21
5.199 ± 0.016.....	19.671 ± 0.005	0.409 ± 0.002	107.7 ± 0.3	0.006	0.004	0.011	...	...	...	...	...	...	...
5.438 ± 0.014.....	19.773 ± 0.004	0.400 ± 0.002	108.0 ± 0.3	0.010	0.023	0.010	...	...	...	...	...	...	...
5.695 ± 0.013.....	19.862 ± 0.007	0.403 ± 0.002	107.8 ± 0.2	−0.002	0.022	0.010	...	...	...	...	...	...	...
5.929 ± 0.014.....	19.958 ± 0.007	0.397 ± 0.002	107.6 ± 0.2	−0.027	0.016	0.010	−0.17	0.08	1.03	−0.03	0.11	−0.26	0.18
6.153 ± 0.016.....	20.060 ± 0.006	0.391 ± 0.002	108.0 ± 0.3	−0.035	0.024	0.011	...	...	...	...	...	...	...
6.363 ± 0.020.....	20.156 ± 0.006	0.389 ± 0.003	108.4 ± 0.3	−0.017	0.031	0.014	...	...	...	...	...	...	...
6.824 ± 0.023.....	20.365 ± 0.008	0.368 ± 0.003	108.0 ± 0.4	0.003	0.015	0.016	...	...	...	...	...	...	...
7.294 ± 0.025.....	20.559 ± 0.010	0.360 ± 0.003	108.1 ± 0.4	−0.002	0.019	0.018	0.12	−0.17	1.74	−0.50	0.46	0.10	0.23
7.837 ± 0.032.....	20.749 ± 0.011	0.369 ± 0.004	108.2 ± 0.5	−0.070	−0.029	0.023	...	...	...	...	...	...	...
8.369 ± 0.056.....	20.905 ± 0.015	0.364 ± 0.006	108.4 ± 0.7	0.017	0.081	0.039	...	...	...	...	...	...	...

TABLE 1—*Continued*

a (arcsec)	μ_R (mag arcsec^{-2})	e	P.A. (deg)	Δx_c (arcsec)	Δy_c (arcsec)	Err.[a] (arcsec)	a_3/a (×100)	b_3/a (×100)	a_4/a (×100)	b_4/a (×100)	a_6/a (×100)	b_6/a (×100)	Err.[b]
					GMP 2440								
8.831 ± 0.073.....	21.088 ± 0.016	0.349 ± 0.008	108.6 ± 1.0	0.009	0.068	0.052	...	...	...	...	...	...	...
9.380 ± 0.088.....	21.272 ± 0.016	0.331 ± 0.009	107.0 ± 1.1	−0.026	0.155	0.062	...	...	...	...	...	...	...
10.130 ± 0.079.....	21.437 ± 0.019	0.336 ± 0.007	107.5 ± 0.9	−0.144	0.146	0.056	...	...	...	...	...	...	...
11.088 ± 0.072.....	21.674 ± 0.017	0.350 ± 0.006	107.2 ± 0.8	−0.109	0.158	0.051	...	...	...	...	...	...	...
11.928 ± 0.082.....	21.888 ± 0.021	0.339 ± 0.006	108.6 ± 0.8	0.050	0.306	0.058	...	...	...	...	...	...	...
12.852 ± 0.119.....	22.021 ± 0.029	0.349 ± 0.008	107.2 ± 1.1	0.144	0.278	0.084	...	...	...	...	...	...	...
13.723 ± 0.145.....	22.144 ± 0.037	0.343 ± 0.010	105.5 ± 1.2	0.256	0.209	0.103	...	...	...	...	...	...	...
14.478 ± 0.206.....	22.245 ± 0.037	0.334 ± 0.013	105.8 ± 1.7	0.054	0.236	0.146	...	...	...	...	...	...	...

NOTE.—Table 1 is also available in machine-readable form in the electronic edition of the *Supplement*.

[a] Error on the center coordinates derived from the residual rms of the ellipse fit to the isophotes, Err $= \mathrm{rms}_{\mathrm{fit}}/\sqrt{N}$, with $N \leq 128$ the number of fitted points of the isophote.

[b] Error of Fourier coefficients defined as Err$= \{[\sum_{i=10}^{N/2}(a_i^2 + b_i^2)]/(N/2 - 10)\}^{1/2}(100/a)$.

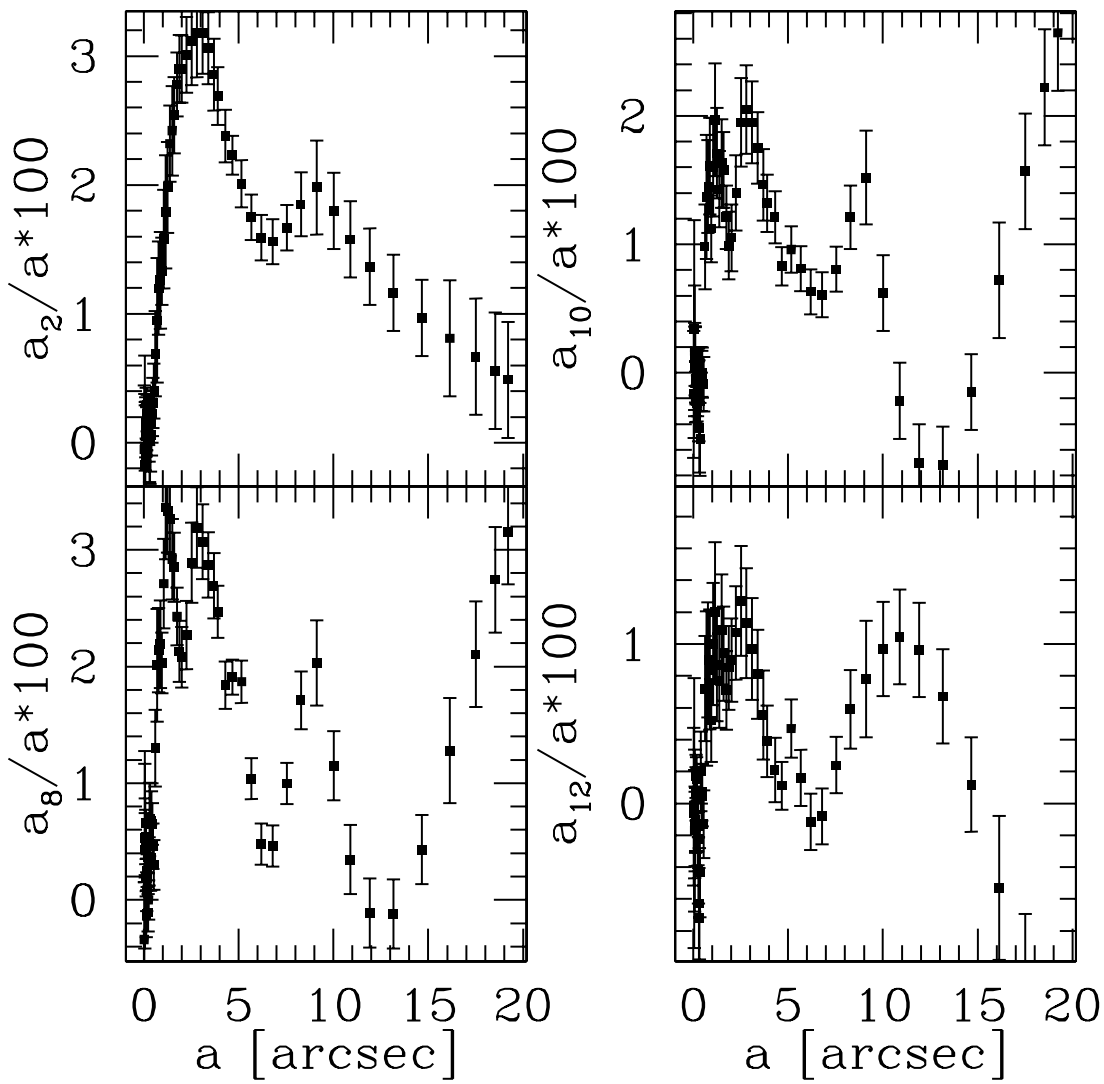

FIG. 2.—Radial profiles of the *R*-band second, eighth, tenth, and twelfth cosine Fourier coefficient (a_2, a_8, a_{10}, and a_{12}) as a function of the semimajor axis distance in arcseconds for the galaxy GMP 1176.

TABLE 2

SECOND-, EIGHTH-, TENTH-, AND TWELFTH-ORDER COSINE FOURIER COEFFICIENTS OF THE ISOPHOTAL SHAPE DECOMPOSITION OF GMP 1176

a (arcsec)	a_2/a (×100)	a_8/a (×100)	a_{10}/a (×100)	a_{12}/a (×100)	a (arcsec)	a_2/a (×100)	a_8/a (×100)	a_{10}/a (×100)	a_{12}/a (×100)
0.015	−0.05	−0.34	−0.17	−0.02	1.489	2.42	2.92	1.63	1.09
0.044	−0.17	0.43	0.34	−0.06	1.604	2.54	2.85	1.58	0.94
0.059	−0.13	0.66	0.17	−0.17	1.741	2.78	2.43	1.21	0.71
0.073	−0.05	0.53	0.05	−0.13	1.874	2.90	2.13	0.99	0.85
0.086	0.05	0.48	0.09	−0.16	2.005	2.90	2.08	1.05	0.90
0.097	0.12	0.54	0.13	−0.16	2.254	3.01	2.27	1.40	1.07
0.111	0.23	−0.12	−0.19	−0.10	2.526	3.12	2.89	1.95	1.27
0.126	0.16	0.19	−0.07	−0.15	2.803	3.18	3.19	2.05	1.13
0.139	0.11	0.07	−0.08	0.06	3.091	3.18	3.07	1.95	0.97
0.154	0.16	0.22	−0.05	0.17	3.391	3.06	2.87	1.75	0.81
0.171	0.23	0.25	0.03	0.15	3.684	2.86	2.69	1.46	0.55
0.193	0.17	0.37	−0.24	0.08	3.889	2.69	2.47	1.32	0.39
0.215	0.15	−0.11	−0.18	−0.14	4.306	2.38	1.84	1.21	0.21
0.239	0.15	0.00	−0.08	−0.22	4.676	2.23	1.91	0.83	0.11
0.266	0.06	0.33	−0.02	−0.42	5.157	2.01	1.87	0.96	0.47
0.293	0.01	0.69	−0.22	−0.72	5.661	1.75	1.04	0.81	0.16
0.322	0.03	0.65	−0.43	−0.63	6.190	1.59	0.48	0.63	−0.12
0.354	0.06	0.36	−0.52	−0.43	6.797	1.56	0.46	0.61	−0.08
0.395	0.15	0.68	−0.05	0.20	7.536	1.67	1.00	0.81	0.24
0.436	0.23	0.65	−0.01	0.07	8.281	1.85	1.71	1.21	0.59
0.481	0.31	0.46	0.00	0.05	9.114	1.98	2.03	1.52	0.78
0.534	0.40	0.30	−0.09	−0.13	10.019	1.80	1.15	0.62	0.97
0.608	0.69	1.30	0.98	0.72	10.898	1.58	0.35	−0.22	1.04
0.692	0.95	2.01	1.37	0.72	11.918	1.37	−0.11	−0.70	0.96
0.779	1.20	2.14	1.45	0.90	13.164	1.16	−0.12	−0.72	0.67
0.866	1.26	2.19	1.61	0.84	14.672	0.97	0.43	−0.15	0.12
0.946	1.33	2.03	1.12	0.52	16.144	0.81	1.28	0.72	−0.53
1.046	1.58	2.71	1.60	1.00	17.500	0.67	2.10	1.57	−1.14
1.148	1.79	3.36	1.97	1.20	18.545	0.56	2.74	2.22	−1.62
1.246	1.98	3.33	1.71	0.87	19.222	0.49	3.15	2.65	−1.92
1.375	2.32	3.26	1.43	0.77	...	...	...	...	...

TABLE 3

LOG OF SPECTROSCOPIC OBSERVATIONS

Object (1)	Run (2)	P.A. (deg) (3)	Position (4)	Offset (arcsec) (5)	Single Exp. Time (s) (6)	Total Exp. Time (hr) (7)	FWHM (8)	Q (arcsec) (9)
GMP 0144	1	46	DG	...	1 × 2700	0.8	2.2	2
	1	1	MN	...	1 × 2700	0.8	1.8	1
GMP 2417	3	55	‖ MJ	3.8 S	6 × 3600	6.0	1.7	3
	3	145	MN	...	3 × 3600	3.0	2.3	3
GMP 2440	1	75	DG	...	1 × 2700	0.8	3.2	2
	1	18	MN	...	1 × 2700	0.8	1.9	2
GMP 2921	5	171	MN	...	3 × 3600	3.0	2.7	2
GMP 3329	5	135	MN	...	3 × 3600	3.0	2.8	3
GMP 3414	3	178	‖ MJ	4.6 N	6 × 3600	6.0	2.5	3
	3	88	MN	...	3 × 3600	3.0	2.5	2
GMP 3958	4	12	MN	...	1130 + 1050	0.6	3.0	3
GMP 4822	5	15	MN	...	1800 + 3 × 3600	3.5	2.8	2
GMP 4928	2	108	DG	...	1 × 3600	1.0	3.2	3
	3	108	DG	...	1829 + 2 × 3600	2.5	2.7	3
	2	153	MN	...	3 × 3600	3.0	2.9	3
GMP 5279	1	146	MN	...	1 × 2700	0.8	1.4	2
GMP 5568	2	78	‖ MJ	2.8 N	3142 + 3 × 3600	3.9	1.6	3
	5	78	‖ MJ	14.0 N	6 × 3600	6.0	2.8	3
	2	168	MN	...	4 × 3600	4.0	2.6	3
	5	168	MN	...	4 × 3600	4.0	2.7	3
GMP 5975	5	68	DG	...	3 × 3600	3.0	2.0	2

NOTE.—Col. (1): GMP No. from Godwin, Metcalfe & Peach (1983). Col. (2): Observing run. Col. (3): Slit position angle measured north through east. Col. (4): Slit position. MJ = major axis; ‖ MJ = parallel to major axis; MN = minor axis; DG = diagonal axis. Col. (5): Northward/southward offset of the slit with respect to galaxy center. Col. (6): Number and exposure time of the single exposures. Col. (7): Total exposure time. Col. (8): FWHM of the seeing and instrumental PSF of the resulting spectrum. Col. (9): Estimated quality of the resulting spectrum. 1: very good; 2: good; 3: medium (see Fig. 3).

TABLE 4
INSTRUMENTAL SETUP OF SPECTROSCOPIC OBSERVATIONS

Parameter	Run 1	Run 2	Run 3	Run 4	Run 5
Telescope	HET	2.4 m Hiltner	2.4 m Hiltner	HET	2.4 m Hiltner
Spectrograph	LRS	Modular	Modular	LRS	Modular
Grating (gr mm^{-1})	Grism G2 600	1200	1200	Echelle E2 316	1200
CCD	Ford Aerospace	"Echelle" SITe	"Echelle" SITe	Ford Aerospace	"Echelle" SITe
Pixel number	3072×3072	2048×2048	2048×2048	3072×3072	2048×2048
Pixel size (μ m^2)	15×15	24×24	24×24	15×15	24×24
Binning	2×2	1×1	1×1	2×2	1×1
Gain (e^-ADU^{-1})	1.8	2.7	2.7	1.8	2.7
RON (e^-)	5.2	7.9	7.9	5.2	7.9
Scale (arcsec pixel^{-1})	0.47	0.606	0.606	0.47	0.606
Dispersion (Å pixel^{-1})	1.99	0.91	1.01	0.72	1.01
Slit width (arcsec)	1.0	1.9	1.9	1.0	1.9
Wavelength range[a] (Å)	4284–7400	4702–6401	4644–6455	4870–5956	4544–6363
Instrumental FWHM (Å)	4.7	2.5	2.3	2.1	2.3
Instrumental σ[b] (km s^{-1})	114	61	53	51	53

[a] Measured on reduced spectra.
[b] Derived at the 5170 Å (corresponding to Mg I triplet).

arc-lamp spectrum. We checked that the wavelength rebinning had been done properly by measuring the difference between the measured and predicted wavelengths for the emission lines in the comparison arc lamp spectra. The rms of the wavelength solution is ~0.10 Å in run 1, ~0.06 Å in runs 2, 3, and 5, and ~0.36 Å in run 4. They correspond to ~6, 3, and 21 km s^{-1} at 5170 Å (i.e., the wavelength of the Mg I absorption triplet), respectively. Systematic errors of the absolute wavelength calibration ($\leq$10 km s^{-1}) were estimated by measuring the difference between the measured and predicted wavelengths (Osterbrock et al. 1996) for the brightest night-sky emission lines in the observed spectral range. The instrumental resolution in each run was derived as the mean of the Gaussian FWHMs measured for a number of unblended arc-lamp lines that were distributed over the whole spectral range of a wavelength-calibrated spectrum. The mean FWHM of the arc-lamp lines and the corresponding instrumental resolution derived at 5170 Å is given in Table 4. In galaxy and stellar spectra the contribution of the sky was determined by interpolating along the outermost 10″–30″ at the two edges of the slit, where the galaxy or stellar light was negligible, and then subtracted. A sky subtraction better than 1% was achieved. All the spectra were corrected for CCD misalignment following Bender et al. (1994). The spectra obtained for the same galaxy along the same axis were co-added using the center of the stellar continuum as reference. This allowed improving the S/N of the resulting two-dimensional spectrum. A one-dimensional spectrum was obtained for each kinematical template star as well as for each flux standard star. The spectra of the kinematical Lick-system templates were deredshifted to laboratory wavelengths. The FWHM of the point-spread function (PSF) due to seeing and instrumental setup is given in Table 3 for the co-added galaxy spectra. It was estimated by comparing the surface-brightness radial profile obtained from each spectrum with the corresponding one extracted from the *HST* WFPC2 *R*-band image of the galaxy. All the profiles are presented in Thomas et al. (2007). Slit width and orientation and WFPC2 PSF were taken into account. The low S/N in the outskirts of the WFPC2 image of GMP 5568 did not allow us to extract a reliable surface-brightness profile to be compared to that of the farthest offset spectrum in the galaxy. The FWHM of this spectrum was derived by interpolating the values of the spectra obtained before and after it. The same is true for the spectra of GMP 3414 and GMP 4822, for which no image was available in the *HST* Science Archive.

4. RESULTS

4.1. *Stellar Kinematics*

The stellar kinematics was measured from the galaxy absorption features present in the wavelength range and centered on the Mg I line triplet ($\lambda\lambda$ 5164, 5173, 5184 Å) by applying the Fourier Correlation Quotient method (Bender 1990) as done by Bender et al. (1994).

The spectra were rebinned along the dispersion direction to natural logarithmic scale, and along the spatial direction to obtain a nearly constant S/N$\geq$20 per resolution element. In a few spectra the S/N decreases to ~10 at the outermost radii. The galaxy continuum was removed row by row by fitting a fourth- to sixth-order polynomial. The quality of the final spectrum depends on the resulting S/N. In Figure 3 we show examples of central spectra covering the three quality classes listed in Table 3. The quality parameter is 1 for S/N $\geq$ 100, 2 for 50 $\leq$ S/N $<$ 100, and 3 for 20 $\leq$ S/N $\leq$ 50.

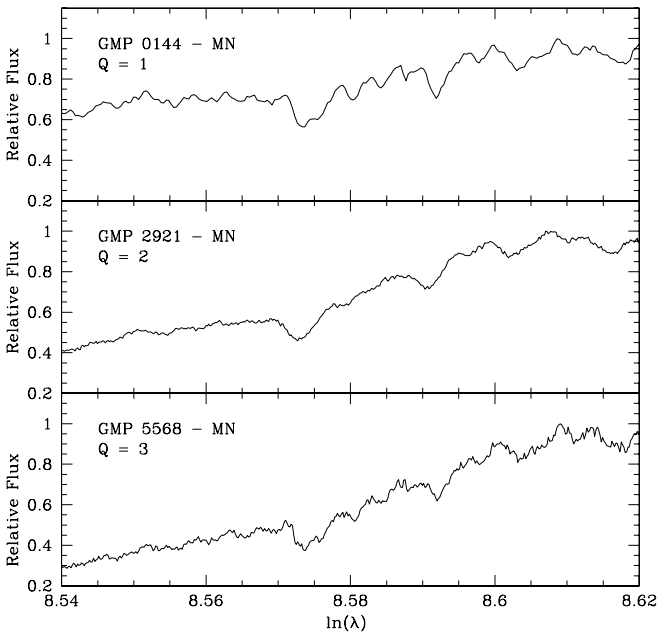

FIG. 3.—Example of central spectra covering the range of quality classes. Relative fluxes have false zero points for viewing convenience.

TABLE 5

STELLAR KINEMATICS OF THE SAMPLE GALAXIES

r (arcsec)	V (km s^{-1})	σ (km s^{-1})	H_3	H_4	P.A. (deg)	Offset (arcsec)	Run
			GMP 0144				
−3.83	−7.9 ± 11.8	248.8 ± 11.3	−0.044 ± 0.039	−0.063 ± 0.034	46	0.0	1
−0.88	−9.9 ± 7.6	244.0 ± 6.8	0.003 ± 0.021	−0.034 ± 0.021	46	0.0	1
0.83	4.8 ± 7.1	237.0 ± 7.7	−0.023 ± 0.026	−0.045 ± 0.025	46	0.0	1
3.90	12.9 ± 16.7	225.3 ± 17.1	−0.008 ± 0.052	−0.082 ± 0.051	46	0.0	1
−13.86	−2.7 ± 15.1	173.9 ± 18.5	0.036 ± 0.079	−0.058 ± 0.080	1	0.0	1
−5.52	−17.6 ± 11.1	229.3 ± 10.7	0.041 ± 0.038	−0.046 ± 0.030	1	0.0	1
−2.37	−7.1 ± 8.3	244.5 ± 6.5	−0.015 ± 0.028	−0.065 ± 0.024	1	0.0	1
−0.79	−3.5 ± 9.1	243.6 ± 7.4	0.009 ± 0.023	−0.053 ± 0.019	1	0.0	1
0.57	0.5 ± 6.9	250.9 ± 5.2	0.023 ± 0.023	−0.068 ± 0.021	1	0.0	1
2.14	3.4 ± 6.7	238.2 ± 6.2	0.004 ± 0.027	−0.087 ± 0.026	1	0.0	1
5.27	10.2 ± 8.0	222.6 ± 7.7	−0.011 ± 0.032	−0.098 ± 0.039	1	0.0	1
13.71	16.9 ± 16.5	202.0 ± 16.0	0.007 ± 0.073	−0.131 ± 0.094	1	0.0	1
			GMP 2417				
−6.92	−90.9 ± 43.7	172.7 ± 42.6	0.014 ± 0.105	−0.096 ± 0.134	55	−3.8	3
−2.56	−87.2 ± 34.1	203.5 ± 39.9	0.001 ± 0.108	−0.059 ± 0.080	55	−3.8	3
1.43	77.7 ± 37.1	217.5 ± 48.6	0.068 ± 0.101	0.027 ± 0.088	55	−3.8	3
6.23	100.5 ± 49.5	175.9 ± 62.1	0.044 ± 0.152	−0.011 ± 0.141	55	−3.8	3
−3.29	−32.1 ± 25.6	175.1 ± 33.0	0.052 ± 0.079	−0.019 ± 0.110	145	0.0	3
−1.84	10.2 ± 14.3	233.4 ± 15.9	−0.014 ± 0.039	−0.026 ± 0.033	145	0.0	3
−1.00	−4.4 ± 11.5	221.0 ± 11.2	−0.004 ± 0.036	−0.089 ± 0.031	145	0.0	3
−0.40	18.4 ± 9.4	237.2 ± 9.9	0.024 ± 0.029	−0.049 ± 0.024	145	0.0	3
0.21	−13.8 ± 9.7	235.8 ± 11.3	0.005 ± 0.030	−0.034 ± 0.026	145	0.0	3
0.81	2.5 ± 11.2	230.0 ± 11.4	0.014 ± 0.034	−0.059 ± 0.029	145	0.0	3
1.66	6.5 ± 12.4	204.2 ± 15.0	−0.051 ± 0.044	−0.088 ± 0.041	145	0.0	3
3.66	13.0 ± 20.6	167.7 ± 21.8	−0.024 ± 0.109	−0.115 ± 0.096	145	0.0	3
			GMP 2440				
−3.00	−123.0 ± 11.0	158.2 ± 12.9	0.072 ± 0.096	−0.020 ± 0.088	75	0.0	1
−0.76	−64.3 ± 7.9	219.3 ± 8.7	0.007 ± 0.038	−0.079 ± 0.056	75	0.0	1
0.35	−0.2 ± 7.7	232.6 ± 8.3	−0.017 ± 0.031	−0.033 ± 0.037	75	0.0	1
1.45	105.0 ± 13.1	193.6 ± 18.3	−0.083 ± 0.056	0.080 ± 0.053	75	0.0	1
4.27	132.7 ± 30.9	145.9 ± 18.2	−0.116 ± 0.121	−0.056 ± 0.126	75	0.0	1
−4.36	−17.0 ± 24.8	183.1 ± 23.4	0.072 ± 0.120	0.016 ± 0.096	18	0.0	1
−1.15	9.0 ± 8.6	222.2 ± 10.0	0.029 ± 0.038	−0.031 ± 0.042	18	0.0	1
0.88	7.0 ± 7.1	224.0 ± 8.2	−0.011 ± 0.032	−0.050 ± 0.042	18	0.0	1
4.06	1.1 ± 28.4	180.5 ± 19.3	−0.044 ± 0.114	−0.072 ± 0.118	18	0.0	1
			GMP 2921				
−11.08	−20.5 ± 52.3	412.8 ± 81.7	−0.015 ± 0.095	0.034 ± 0.094	171	0.0	5
−5.90	12.5 ± 13.1	356.2 ± 17.0	0.007 ± 0.024	0.038 ± 0.029	171	0.0	5
−2.60	1.3 ± 10.2	391.5 ± 14.3	0.004 ± 0.018	0.030 ± 0.022	171	0.0	5
−1.16	11.7 ± 7.5	399.4 ± 10.4	0.017 ± 0.013	0.026 ± 0.016	171	0.0	5
0.03	10.4 ± 6.5	390.3 ± 8.3	−0.001 ± 0.012	−0.003 ± 0.014	171	0.0	5
1.21	−5.4 ± 9.1	383.9 ± 8.0	0.023 ± 0.015	−0.022 ± 0.012	171	0.0	5
2.65	−8.6 ± 8.7	384.7 ± 11.4	0.008 ± 0.016	0.003 ± 0.019	171	0.0	5
5.76	−4.6 ± 15.3	414.0 ± 18.2	−0.006 ± 0.025	0.018 ± 0.021	171	0.0	5
10.76	3.3 ± 45.8	388.1 ± 63.8	0.019 ± 0.072	0.001 ± 0.054	171	0.0	5
			GMP 3329				
−9.50	−17.3 ± 35.9	269.3 ± 58.7	0.008 ± 0.081	0.049 ± 0.073	135	0.0	5
−4.86	6.8 ± 12.6	246.5 ± 16.0	0.010 ± 0.029	−0.009 ± 0.034	135	0.0	5
−2.55	−0.9 ± 8.7	272.3 ± 11.5	0.000 ± 0.020	−0.007 ± 0.022	135	0.0	5
−1.08	1.8 ± 8.3	268.6 ± 9.8	−0.004 ± 0.018	−0.025 ± 0.025	135	0.0	5
0.11	−7.1 ± 7.9	280.3 ± 10.9	0.002 ± 0.019	−0.028 ± 0.028	135	0.0	5
1.31	2.9 ± 7.8	269.4 ± 10.9	−0.020 ± 0.020	−0.025 ± 0.027	135	0.0	5
2.78	5.2 ± 8.4	243.1 ± 10.5	0.003 ± 0.020	−0.029 ± 0.025	135	0.0	5
5.08	3.1 ± 9.6	219.9 ± 15.0	−0.012 ± 0.036	−0.050 ± 0.032	135	0.0	5
9.56	5.8 ± 33.2	274.5 ± 31.5	−0.056 ± 0.058	−0.087 ± 0.053	135	0.0	5

TABLE 5—*Continued*

r (arcsec)	V (km s^{-1})	σ (km s^{-1})	H_3	H_4	P.A. (deg)	Offset (arcsec)	Run
			GMP 3414				
−6.88	−88.3 ± 37.3	92.6 ± 56.9	0.079 ± 0.214	−0.119 ± 0.206	178	4.6	3
−2.47	−49.2 ± 31.1	158.7 ± 34.3	0.004 ± 0.094	−0.158 ± 0.088	178	4.6	3
1.56	33.4 ± 34.8	159.8 ± 34.9	0.001 ± 0.143	−0.083 ± 0.093	178	4.6	3
6.01	104.1 ± 49.7	130.8 ± 74.2	−0.183 ± 0.259	0.035 ± 0.102	178	4.6	3
−2.99	11.8 ± 22.1	158.0 ± 22.8	0.018 ± 0.111	−0.129 ± 0.058	88	0.0	3
−1.25	14.1 ± 10.6	172.1 ± 7.2	0.011 ± 0.033	−0.072 ± 0.028	88	0.0	3
−0.41	9.1 ± 8.4	167.9 ± 5.5	0.019 ± 0.028	−0.086 ± 0.025	88	0.0	3
0.20	2.7 ± 8.1	178.1 ± 6.3	0.018 ± 0.030	−0.058 ± 0.023	88	0.0	3
0.81	3.9 ± 8.4	159.4 ± 9.2	0.035 ± 0.043	−0.011 ± 0.029	88	0.0	3
1.65	−14.4 ± 8.1	168.1 ± 9.6	−0.002 ± 0.027	−0.070 ± 0.031	88	0.0	3
3.27	−26.9 ± 17.3	133.8 ± 20.2	0.068 ± 0.106	−0.099 ± 0.061	88	0.0	3
			GMP 3958				
−2.94	−4.0 ± 26.7	202.0 ± 30.8	0.069 ± 0.079	0.010 ± 0.061	12	0.0	4
−1.82	12.6 ± 11.9	157.4 ± 13.5	−0.007 ± 0.045	−0.063 ± 0.033	12	0.0	4
−0.89	−4.1 ± 9.2	161.0 ± 8.8	0.048 ± 0.035	−0.117 ± 0.032	12	0.0	4
0.03	−0.4 ± 6.7	144.5 ± 6.9	0.027 ± 0.029	−0.102 ± 0.029	12	0.0	4
0.96	−7.5 ± 6.9	143.3 ± 7.2	0.038 ± 0.030	−0.086 ± 0.029	12	0.0	4
1.88	5.6 ± 11.6	160.8 ± 10.5	0.030 ± 0.044	−0.099 ± 0.039	12	0.0	4
3.00	−1.9 ± 13.0	145.5 ± 15.3	0.080 ± 0.054	−0.086 ± 0.039	12	0.0	4
			GMP 4822				
−5.69	12.7 ± 15.8	237.2 ± 25.1	0.089 ± 0.056	−0.005 ± 0.053	15	0.0	5
−2.77	−4.2 ± 7.2	240.2 ± 9.5	0.029 ± 0.023	0.001 ± 0.024	15	0.0	5
−1.34	−2.3 ± 4.9	250.0 ± 7.1	0.038 ± 0.016	0.019 ± 0.017	15	0.0	5
−0.47	4.0 ± 4.9	246.1 ± 6.4	0.027 ± 0.016	−0.016 ± 0.017	15	0.0	5
0.14	1.9 ± 4.5	253.9 ± 6.1	0.040 ± 0.014	−0.013 ± 0.015	15	0.0	5
0.75	2.6 ± 5.1	253.9 ± 7.5	0.025 ± 0.016	−0.003 ± 0.017	15	0.0	5
1.61	−3.2 ± 5.7	254.4 ± 6.5	0.012 ± 0.016	−0.009 ± 0.018	15	0.0	5
3.06	−7.5 ± 6.6	248.2 ± 10.0	0.029 ± 0.021	0.000 ± 0.022	15	0.0	5
6.00	−3.7 ± 16.5	253.9 ± 18.6	0.005 ± 0.031	0.009 ± 0.036	15	0.0	5
			GMP 4928				
−3.64	−16.2 ± 45.3	296.0 ± 61.9	0.046 ± 0.100	−0.024 ± 0.078	108	0.0	2
−1.38	−0.8 ± 39.3	334.5 ± 63.7	0.047 ± 0.086	0.111 ± 0.102	108	0.0	2
0.05	19.5 ± 21.2	307.1 ± 36.8	0.005 ± 0.052	0.060 ± 0.048	108	0.0	2
1.48	18.8 ± 24.8	293.5 ± 26.1	0.025 ± 0.055	−0.006 ± 0.047	108	0.0	2
3.75	−21.2 ± 50.0	317.5 ± 69.3	−0.079 ± 0.099	−0.003 ± 0.068	108	0.0	2
−4.56	15.5 ± 32.7	278.0 ± 44.2	−0.001 ± 0.084	−0.049 ± 0.088	108	0.0	3
−2.03	14.4 ± 14.3	275.0 ± 14.9	0.023 ± 0.038	−0.021 ± 0.034	108	0.0	3
−0.60	−6.0 ± 11.8	293.0 ± 14.3	0.005 ± 0.030	−0.002 ± 0.032	108	0.0	3
0.57	−1.8 ± 9.3	293.5 ± 11.2	0.003 ± 0.025	−0.008 ± 0.027	108	0.0	3
2.00	−10.5 ± 14.0	285.1 ± 14.0	0.037 ± 0.041	−0.042 ± 0.041	108	0.0	3
4.52	−11.4 ± 29.3	277.5 ± 36.4	0.105 ± 0.096	−0.043 ± 0.083	108	0.0	3
−3.40	−36.7 ± 35.3	292.4 ± 48.5	0.035 ± 0.084	−0.032 ± 0.059	153	0.0	2
−2.45	−18.4 ± 15.2	279.5 ± 21.7	−0.028 ± 0.043	−0.019 ± 0.033	153	0.0	2
−1.58	14.2 ± 15.3	282.9 ± 23.2	0.004 ± 0.043	−0.004 ± 0.039	153	0.0	2
−0.97	1.5 ± 11.1	301.5 ± 17.5	−0.003 ± 0.033	−0.033 ± 0.032	153	0.0	2
−0.37	−6.7 ± 10.8	288.6 ± 16.7	−0.018 ± 0.033	−0.020 ± 0.028	153	0.0	2
0.24	12.0 ± 11.3	295.2 ± 17.7	0.004 ± 0.032	−0.044 ± 0.031	153	0.0	2
0.85	13.2 ± 12.6	257.7 ± 15.4	−0.007 ± 0.040	−0.060 ± 0.037	153	0.0	2
1.71	16.5 ± 15.0	270.9 ± 20.0	0.034 ± 0.040	−0.023 ± 0.036	153	0.0	2
2.93	4.7 ± 21.3	267.0 ± 28.1	0.027 ± 0.064	−0.081 ± 0.050	153	0.0	2
			GMP 5279				
−9.26	−3.2 ± 32.3	257.1 ± 37.2	−0.094 ± 0.075	−0.032 ± 0.053	146	0.0	1
−2.78	−3.0 ± 11.2	281.9 ± 7.7	−0.009 ± 0.031	−0.066 ± 0.028	146	0.0	1
−0.69	−1.4 ± 9.1	280.8 ± 7.3	−0.013 ± 0.024	−0.025 ± 0.020	146	0.0	1
0.64	−1.1 ± 10.2	292.2 ± 8.0	−0.054 ± 0.026	−0.038 ± 0.022	146	0.0	1
2.64	5.3 ± 10.3	271.8 ± 7.9	−0.009 ± 0.024	−0.049 ± 0.026	146	0.0	1
8.38	3.7 ± 25.4	246.7 ± 26.5	−0.027 ± 0.075	−0.092 ± 0.072	146	0.0	1

TABLE 5—*Continued*

r (arcsec)	V (km s^{-1})	σ (km s^{-1})	H_3	H_4	P.A. (deg)	Offset (arcsec)	Run
			GMP 5568				
−4.60	1.2 ± 25.0	255.1 ± 28.2	−0.038 ± 0.075	−0.085 ± 0.069	78	2.8	2
−2.05	2.1 ± 19.6	264.6 ± 19.6	0.066 ± 0.053	0.003 ± 0.047	78	2.8	2
−0.60	−1.1 ± 15.1	263.9 ± 19.3	−0.005 ± 0.040	0.026 ± 0.039	78	2.8	2
0.58	−18.2 ± 10.2	228.2 ± 15.2	−0.005 ± 0.043	−0.014 ± 0.038	78	2.8	2
2.03	6.0 ± 14.0	235.4 ± 19.3	0.016 ± 0.056	−0.041 ± 0.049	78	2.8	2
4.57	10.0 ± 33.4	259.7 ± 39.6	0.026 ± 0.079	−0.080 ± 0.067	78	2.8	2
−4.88	−12.1 ± 133.3	277.3 ± 95.5	−0.018 ± 0.095	−0.137 ± 0.099	78	14.0	5
−1.26	8.6 ± 67.8	259.0 ± 98.0	0.094 ± 0.115	−0.073 ± 0.098	78	14.0	5
6.29	−8.6 ± 109.4	280.4 ± 93.2	0.077 ± 0.153	−0.081 ± 0.136	78	14.0	5
2.66	12.3 ± 83.1	317.1 ± 67.1	−0.029 ± 0.120	−0.064 ± 0.102	78	14.0	5
−4.08	6.0 ± 29.8	221.7 ± 46.7	−0.070 ± 0.096	0.004 ± 0.068	168	0.0	2
−2.20	11.7 ± 13.8	256.4 ± 21.7	0.023 ± 0.047	0.003 ± 0.038	168	0.0	2
−1.36	2.3 ± 14.7	257.2 ± 21.0	0.035 ± 0.052	−0.028 ± 0.042	168	0.0	2
−0.75	9.4 ± 8.2	248.7 ± 10.8	−0.014 ± 0.034	−0.040 ± 0.029	168	0.0	2
−0.14	5.9 ± 7.0	252.8 ± 9.5	0.005 ± 0.030	−0.053 ± 0.028	168	0.0	2
0.46	4.0 ± 9.5	265.3 ± 14.1	−0.004 ± 0.034	−0.026 ± 0.032	168	0.0	2
1.07	−14.2 ± 11.4	240.1 ± 16.3	0.012 ± 0.045	−0.026 ± 0.037	168	0.0	2
1.91	−3.3 ± 14.6	237.6 ± 21.8	−0.025 ± 0.055	0.001 ± 0.047	168	0.0	2
3.80	−21.5 ± 29.9	234.1 ± 40.5	−0.060 ± 0.103	−0.081 ± 0.066	168	0.0	2
−3.77	9.9 ± 25.5	262.1 ± 35.1	0.031 ± 0.054	−0.039 ± 0.070	168	0.0	5
−2.31	3.3 ± 12.6	238.2 ± 22.5	−0.001 ± 0.039	0.023 ± 0.047	168	0.0	5
−1.47	16.3 ± 13.2	265.9 ± 19.1	−0.020 ± 0.033	−0.018 ± 0.042	168	0.0	5
−0.86	10.2 ± 11.5	253.0 ± 16.4	0.008 ± 0.033	−0.031 ± 0.039	168	0.0	5
−0.26	−4.5 ± 10.7	253.5 ± 12.7	−0.004 ± 0.028	−0.035 ± 0.030	168	0.0	5
0.35	−0.8 ± 12.4	260.5 ± 13.6	−0.003 ± 0.027	−0.026 ± 0.033	168	0.0	5
0.96	−17.7 ± 12.0	235.6 ± 19.3	−0.011 ± 0.037	0.004 ± 0.041	168	0.0	5
1.80	−22.5 ± 19.9	266.8 ± 26.9	−0.005 ± 0.047	−0.015 ± 0.054	168	0.0	5
3.50	5.7 ± 28.8	238.7 ± 40.4	0.011 ± 0.057	−0.002 ± 0.078	168	0.0	5
			GMP 5975				
−8.13	−104.4 ± 15.0	155.7 ± 12.4	0.125 ± 0.078	−0.218 ± 0.134	68	0.0	5
−3.89	−64.5 ± 9.1	163.3 ± 9.7	0.065 ± 0.028	−0.039 ± 0.048	68	0.0	5
−2.01	−50.0 ± 5.8	199.8 ± 6.5	0.010 ± 0.021	−0.089 ± 0.027	68	0.0	5
−1.17	−25.7 ± 4.1	205.4 ± 5.7	−0.032 ± 0.014	−0.056 ± 0.019	68	0.0	5
−0.57	−13.4 ± 3.3	207.1 ± 4.7	−0.005 ± 0.012	−0.051 ± 0.016	68	0.0	5
0.04	4.0 ± 2.9	208.0 ± 4.1	−0.028 ± 0.010	−0.043 ± 0.014	68	0.0	5
0.65	33.1 ± 4.5	201.7 ± 4.3	−0.038 ± 0.013	−0.027 ± 0.016	68	0.0	5
1.25	42.1 ± 4.0	197.2 ± 5.4	−0.007 ± 0.015	−0.048 ± 0.020	68	0.0	5
2.09	45.4 ± 11.2	213.1 ± 16.1	−0.028 ± 0.035	−0.054 ± 0.032	68	0.0	5
3.99	65.4 ± 8.6	221.6 ± 11.8	−0.016 ± 0.027	−0.063 ± 0.025	68	0.0	5
7.82	67.9 ± 16.0	190.4 ± 20.8	−0.016 ± 0.061	−0.151 ± 0.062	68	0.0	5

NOTE.—Table 5 is also available in machine-readable form in the electronic edition of the *Supplement*.

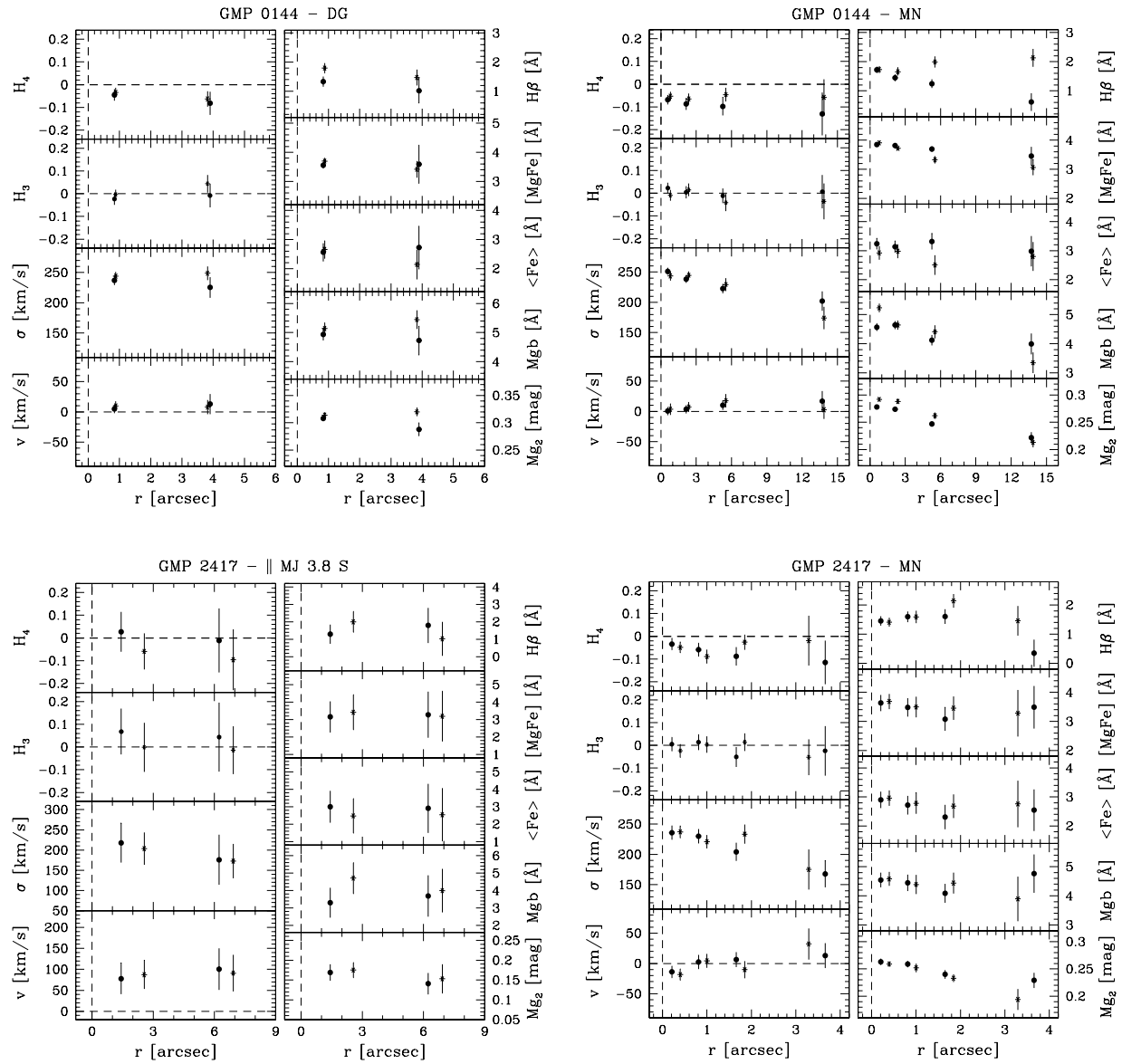

FIG. 4.—Kinematical parameters and line indices measured along the observed axes of the sample galaxies. For each axis the curves are folded around the nucleus. Circles and asterisks (or squares) refer to data measured along the receding and approaching side, respectively. The radial profiles of the line-of-sight velocity (v) after the subtraction of systemic velocity, velocity dispersion (σ), and third (H_3) and fourth (H_4) order coefficient of the Gauss-Hermite decomposition of the LOSVD are shown in the left panels (*from top to bottom*). The radial profiles of the line indices Hβ, [MgFe], $\langle$Fe$\rangle$, Mg b, and Mg_2 are plotted in the right panels (*from top to bottom*). For GMP 4928 open and filled symbols refer to data measured from spectra obtained in run 2 and 3, respectively. For GMP 5568 open and filled symbols refer to data measured from spectra obtained in runs 2 and 5, respectively.

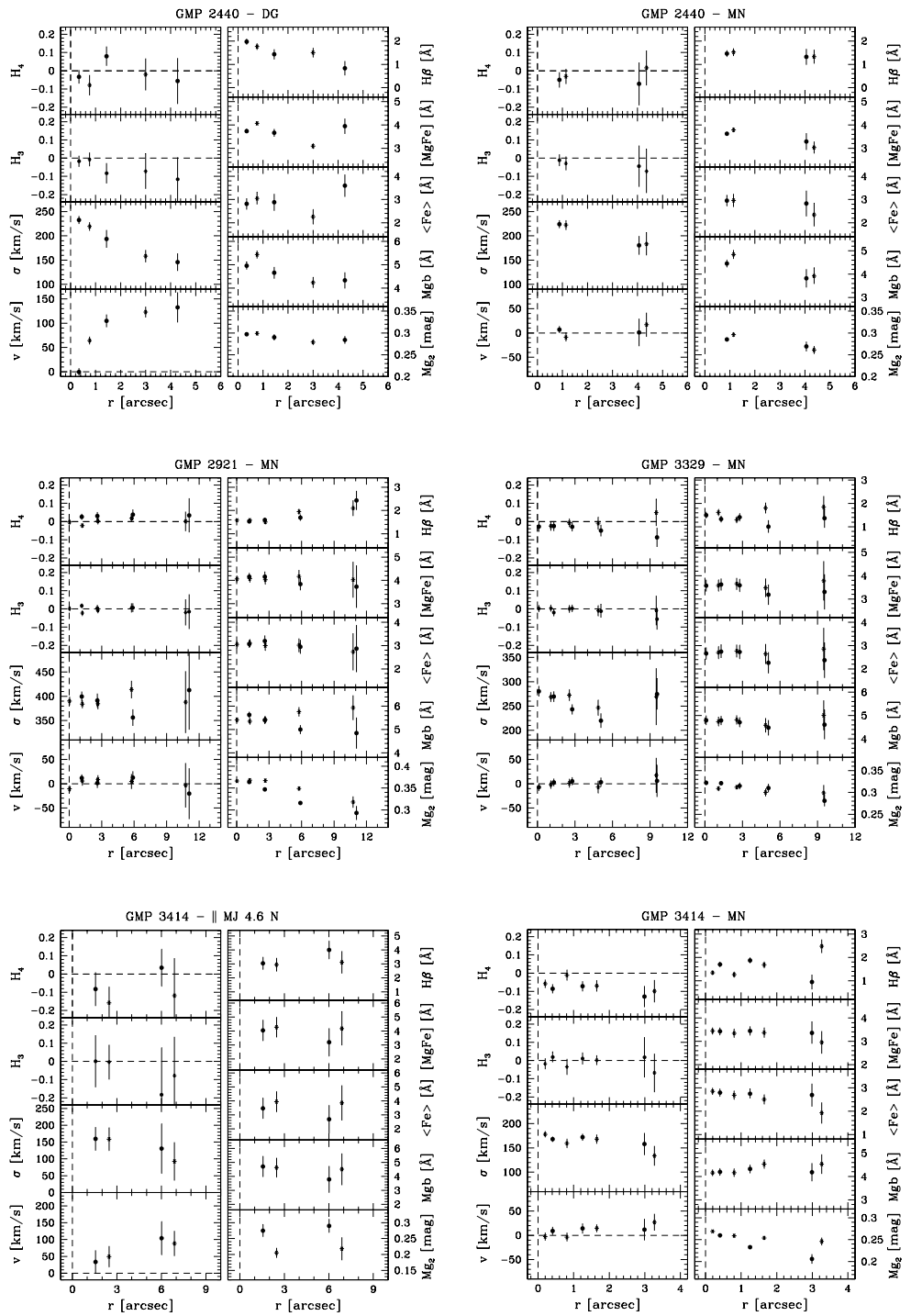

FIG. 4 — *Continued*

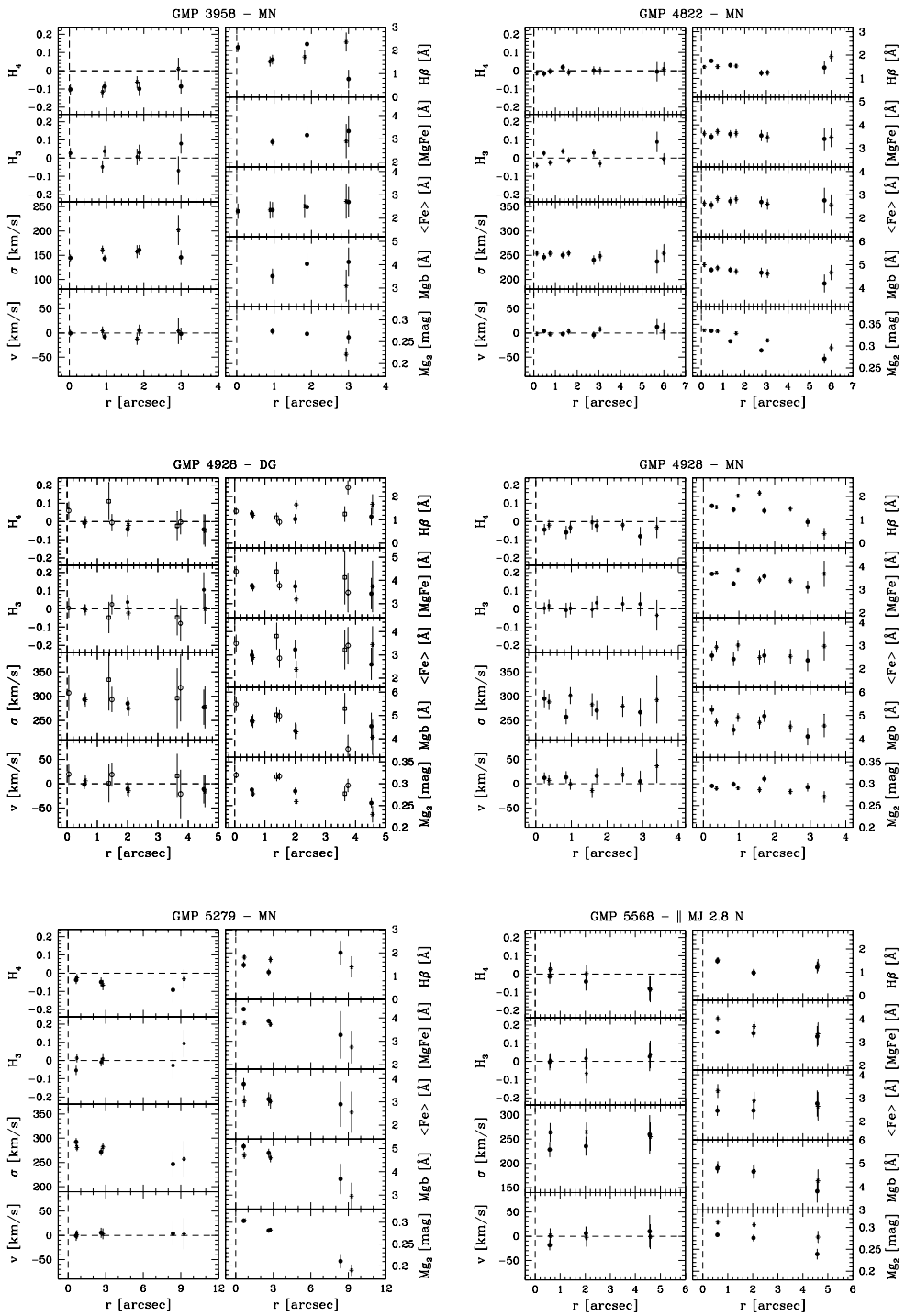

FIG. 4 — *Continued*

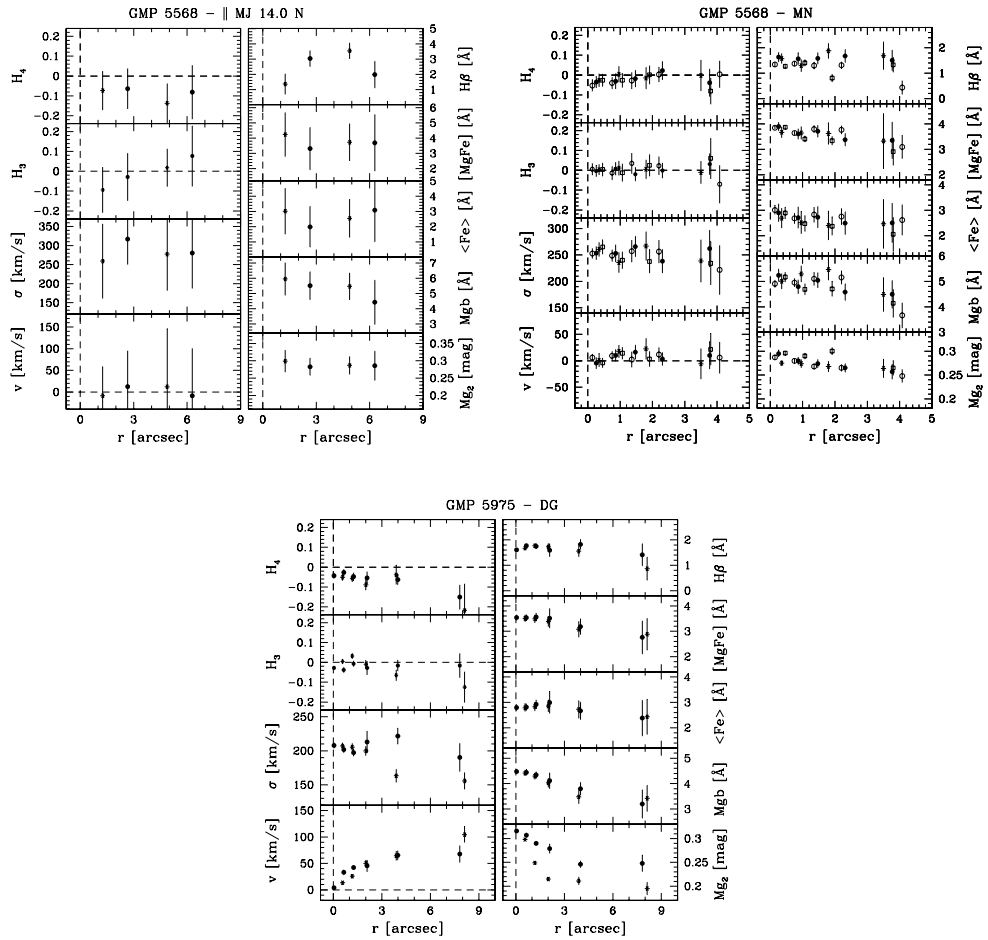

FIG. 4—*Continued*

To measure the stellar kinematics of the sample galaxies we adopted HR 6817 (K1 III) as kinematical template for run 1, HR 6018 (K1 III) for run 2, and HR 3427 (K0 III) for runs 3–5. We derived for each galaxy spectrum the LOSVD along the slit and measured its moments, namely, the line-of-sight radial velocity v, velocity dispersion σ, and values of the coefficients H_3 and H_4. At each radius, they have been derived by fitting the LOSVD with a Gaussian plus third- and fourth-order Gauss-Hermite polynomials $\mathcal{H}_3$ and $\mathcal{H}_4$, which describe the asymmetric and symmetric deviations of the LOSVD from a pure Gaussian profile (van der Marel & Franx 1993; Gerhard 1993). Errors on the LOSVD moments were derived from photon statistics and CCD readout noise, calibrating them by Monte Carlo simulations as done by Bender et al. (1994). In general, errors are in the range of 3–10 km s^{-1} for v and σ, and 0.01–0.04 for H_3 and H_4, becoming larger in the outer parts of some galaxies where $10 \lesssim \mathrm{S/N} < 20$. The largest errors are observed for offset spectra of GMP 2417, GMP 3414, and GMP 5568 with S/N $\approx$ 20. These errors do not take into account possible systematic effects due to template mismatch or the presence of dust and/or faint emission. The measured stellar kinematics is reported in Table 5 and plotted in Figure 4, where profiles folded with respect to, and velocities relative to, the galaxy centers are given.

Figure 5 shows the comparison between the measurements of v, σ, H_3, and H_4 along the minor axis of GMP 0144 obtained here and measurements of Paper II. There is a significant difference in velocity dispersions within 3″ that can be only partially attributed to the different instrumental setup and seeing of the observing runs. The same is true for the velocity dispersion observed along

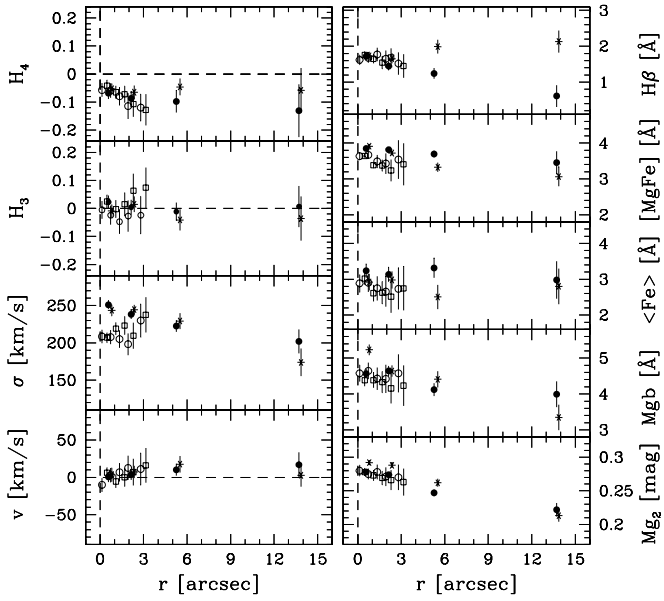

FIG. 5.—Kinematical parameters (*left panels*) and line strength indices profiles (*right panels*) along the minor axis of GMP 0144 measured in run 1 (*filled symbols*) and in Paper II (*open symbols*). Circles refer to data measured along the receding side of the galaxy.

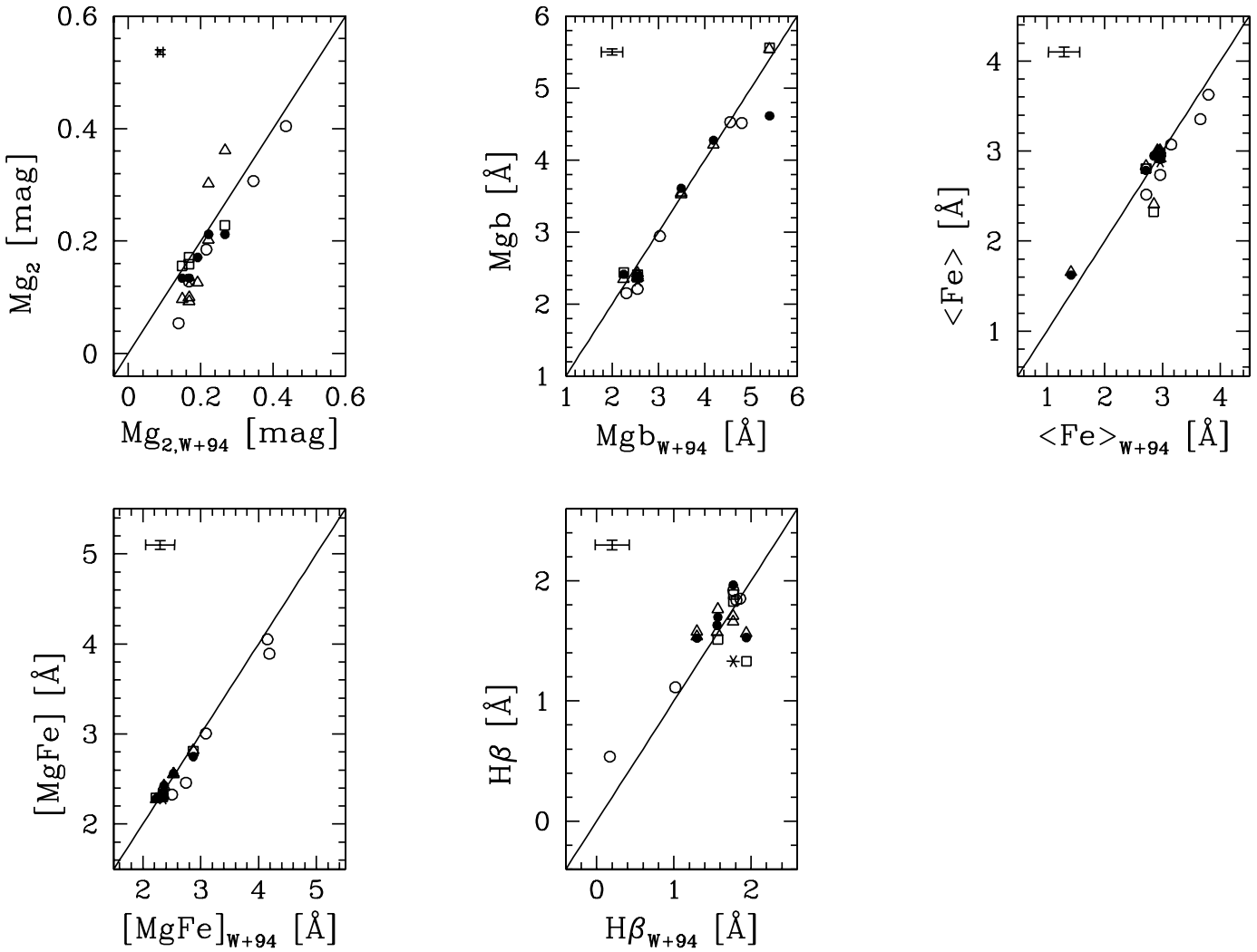

FIG. 6.—Comparison of the values for the line strength indices of Mg_2, Mg b, Mg_2, $\langle Fe\rangle$, [MgFe], and Hβ measured for a sample of stars in this work and in Worthey et al. (1994) W+94. The open circles, filled circles, squares, asterisks, and triangles refer to data obtained in runs 1, 2, 3, 4, and 5, respectively. In each panel the error bars in the upper left corner indicate the mean errors, and the solid line shows the line of correspondence.

the diagonal (Fig. 4) and major axes (Paper I). A likely explanation for the mismatch is that GMP 0144 deviates significantly from axisymmetry near its center and hosts a dynamically hot, decoupled component (Thomas 2006; Thomas et al. 2007). Further observational support for this comes from the relatively large side-to-side asymmetries in all the measured slits and the strong isophotal twist ($\sim 30^\circ$) measured in the very center from *HST* WFPC2 imaging (Paper I).

The multiple observations of GMP 4928 and GMP 5568 agree within the errors.

4.2. *Line Strength Indices*

We measured the Mg, Fe, and Hβ line strength indices following Faber et al. (1985) and Worthey et al. (1994) from flux-calibrated spectra, as done in Papers I and II. Spectra were rebinned in dispersion direction as well as in radial direction as before. We indicate the average iron index with $\langle Fe\rangle = (Fe_{5270} + Fe_{5335})/2$ (Gorgas et al. 1990) and the usual combined magnesium-iron index with $[MgFe] = (Mg\ b\langle Fe\rangle)^{1/2}$ (González 1993). We corrected all the measured indices for velocity dispersion broadening and calibrated our measurements to the Lick system using stars from Worthey et al. (1994, Fig. 6). No zero-point correction was applied since data did not show offset with respect to the Lick system. No focus correction was applied because atmospheric seeing was the dominant effect during observations (see Mehlert et al. 1998 for details). Errors on indices were derived from photon statistics and CCD readout noise, and calibrated by means of Monte Carlo simulations.

The strongest emission feature in the observed spectral range is the [O III] 5007 Å emission line. It falls on top of the Fe_{5015} iron index that we neglected, and it is connected to the Hβ emission line (Osterbrock 1989). By adopting the index definition by González (1993), the equivalent width of the [O III] 5007 Å emission line fell below the detection limit in all but a few of the spectra, namely, those obtained along the minor axes of GMP 2921, GMP 3329, and GMP 4822, and along the diagonal axes of GMP 2440 and GMP 4928. Even in these spectra the [O III] 5007 Å equivalent width was $\lesssim 0.5$ Å. This would correspond to a correction $\lesssim 0.3$ Å for the equivalent width of Hβ. Since it is typically smaller than the statistical errors on Hβ measurements, no correction for emission was applied.

The measured values of Hβ, [MgFe], $\langle Fe\rangle$, Mg b, and Mg_2 are listed in Table 6 and plotted in Figure 4. Figure 5 shows the comparison between the measurements of Hβ, [MgFe], $\langle Fe\rangle$, Mg_2, and Mg b along the minor axis of GMP 0144 obtained here and measurements obtained in Paper II. The values derived from the

TABLE 6

LINE STRENGTH INDICES OF THE SAMPLE GALAXIES

r (arcsec)	Hβ (Å)	[MgFe] (Å)	$\langle$Fe$\rangle$ (Å)	Mg b (Å)	Mg_2 (mag)	P.A. (deg)	Offset (arcsec)	Run
			GMP 0144					
−3.83	1.471 ± 0.276	3.414 ± 0.284	2.140 ± 0.512	5.446 ± 0.325	0.320 ± 0.008	46	0.0	1
−0.88	1.794 ± 0.165	3.696 ± 0.110	2.656 ± 0.305	5.141 ± 0.196	0.314 ± 0.005	46	0.0	1
0.83	1.330 ± 0.175	3.555 ± 0.113	2.560 ± 0.312	4.936 ± 0.204	0.308 ± 0.005	46	0.0	1
3.90	1.014 ± 0.427	3.589 ± 0.663	2.725 ± 0.740	4.727 ± 0.499	0.288 ± 0.012	46	0.0	1
−13.86	2.131 ± 0.305	3.062 ± 0.268	2.802 ± 0.494	3.346 ± 0.355	0.213 ± 0.009	1	0.0	1
−5.52	1.989 ± 0.191	3.325 ± 0.128	2.507 ± 0.337	4.410 ± 0.228	0.262 ± 0.006	1	0.0	1
−2.37	1.652 ± 0.132	3.720 ± 0.071	2.982 ± 0.242	4.642 ± 0.158	0.288 ± 0.004	1	0.0	1
−0.79	1.729 ± 0.120	3.910 ± 0.067	2.923 ± 0.234	5.232 ± 0.147	0.292 ± 0.004	1	0.0	1
0.57	1.719 ± 0.102	3.846 ± 0.044	3.236 ± 0.187	4.571 ± 0.123	0.278 ± 0.003	1	0.0	1
2.14	1.444 ± 0.113	3.817 ± 0.052	3.138 ± 0.203	4.642 ± 0.135	0.274 ± 0.003	1	0.0	1
5.27	1.243 ± 0.152	3.695 ± 0.092	3.312 ± 0.273	4.123 ± 0.183	0.247 ± 0.005	1	0.0	1
13.71	0.610 ± 0.304	3.451 ± 0.323	2.981 ± 0.525	3.995 ± 0.357	0.222 ± 0.010	1	0.0	1
			GMP 2417					
−6.92	1.025 ± 0.961	3.189 ± 1.436	2.545 ± 1.507	3.996 ± 1.231	0.153 ± 0.036	55	−3.8	3
−2.56	1.999 ± 0.597	3.417 ± 1.007	2.478 ± 0.991	4.713 ± 0.893	0.175 ± 0.019	55	−3.8	3
1.43	1.292 ± 0.553	3.153 ± 0.890	3.007 ± 0.914	3.306 ± 0.861	0.169 ± 0.021	55	−3.8	3
6.23	1.798 ± 1.007	3.278 ± 1.320	2.912 ± 1.411	3.690 ± 1.185	0.141 ± 0.027	55	−3.8	3
−3.29	1.459 ± 0.511	3.279 ± 0.799	2.760 ± 0.800	3.896 ± 0.768	0.194 ± 0.019	145	0.0	3
−1.84	2.145 ± 0.234	3.453 ± 0.404	2.685 ± 0.408	4.439 ± 0.364	0.233 ± 0.007	145	0.0	3
−1.00	1.590 ± 0.212	3.495 ± 0.354	2.781 ± 0.356	4.391 ± 0.329	0.252 ± 0.008	145	0.0	3
−0.40	1.408 ± 0.155	3.684 ± 0.262	2.961 ± 0.267	4.582 ± 0.239	0.259 ± 0.005	145	0.0	3
0.21	1.455 ± 0.163	3.631 ± 0.277	2.901 ± 0.282	4.545 ± 0.250	0.263 ± 0.006	145	0.0	3
0.81	1.597 ± 0.185	3.478 ± 0.316	2.720 ± 0.321	4.448 ± 0.284	0.259 ± 0.006	145	0.0	3
1.66	1.604 ± 0.250	3.074 ± 0.402	2.312 ± 0.421	4.086 ± 0.327	0.240 ± 0.008	145	0.0	3
3.66	0.344 ± 0.463	3.485 ± 0.731	2.549 ± 0.715	4.764 ± 0.662	0.229 ± 0.014	145	0.0	3
			GMP 2440					
−3.00	1.504 ± 0.197	3.093 ± 0.108	2.258 ± 0.315	4.236 ± 0.222	0.279 ± 0.006	75	0.0	1
−0.76	1.764 ± 0.143	4.069 ± 0.088	3.044 ± 0.256	5.438 ± 0.169	0.299 ± 0.005	75	0.0	1
0.35	1.974 ± 0.132	3.735 ± 0.073	2.813 ± 0.245	4.958 ± 0.160	0.297 ± 0.004	75	0.0	1
1.45	1.431 ± 0.217	3.662 ± 0.166	2.881 ± 0.365	4.655 ± 0.249	0.290 ± 0.007	75	0.0	1
4.27	0.832 ± 0.307	3.946 ± 0.329	3.597 ± 0.479	4.330 ± 0.348	0.284 ± 0.009	75	0.0	1
−4.36	1.331 ± 0.301	3.030 ± 0.256	2.343 ± 0.495	3.918 ± 0.342	0.261 ± 0.009	18	0.0	1
−1.15	1.524 ± 0.156	3.787 ± 0.095	2.962 ± 0.274	4.842 ± 0.183	0.296 ± 0.005	18	0.0	1
0.88	1.463 ± 0.130	3.625 ± 0.064	2.950 ± 0.230	4.456 ± 0.154	0.285 ± 0.004	18	0.0	1
4.06	1.323 ± 0.346	3.287 ± 0.359	2.829 ± 0.550	3.819 ± 0.397	0.269 ± 0.011	18	0.0	1
			GMP 2921					
−11.08	2.430 ± 0.411	3.732 ± 0.913	2.872 ± 1.009	4.848 ± 0.670	0.293 ± 0.016	171	0.0	5
−5.90	1.692 ± 0.137	3.841 ± 0.268	2.951 ± 0.298	4.999 ± 0.193	0.316 ± 0.004	171	0.0	5
−2.60	1.590 ± 0.104	4.156 ± 0.222	3.197 ± 0.244	5.403 ± 0.165	0.347 ± 0.004	171	0.0	5
−1.16	1.532 ± 0.075	4.158 ± 0.163	3.070 ± 0.167	5.631 ± 0.134	0.364 ± 0.003	171	0.0	5
0.03	1.584 ± 0.066	4.063 ± 0.143	3.049 ± 0.155	5.413 ± 0.105	0.366 ± 0.003	171	0.0	5
1.21	1.582 ± 0.073	4.079 ± 0.159	3.108 ± 0.162	5.353 ± 0.139	0.368 ± 0.003	171	0.0	5
2.65	1.507 ± 0.092	4.032 ± 0.197	3.000 ± 0.214	5.419 ± 0.143	0.367 ± 0.004	171	0.0	5
5.76	1.948 ± 0.123	4.169 ± 0.277	3.016 ± 0.294	5.761 ± 0.203	0.349 ± 0.005	171	0.0	5
10.76	2.100 ± 0.338	4.030 ± 0.769	2.736 ± 0.798	5.936 ± 0.535	0.318 ± 0.013	171	0.0	5
			GMP 3329					
−9.50	1.847 ± 0.475	3.781 ± 0.845	2.853 ± 0.908	5.010 ± 0.645	0.299 ± 0.018	135	0.0	5
−4.86	1.807 ± 0.231	3.481 ± 0.398	2.644 ± 0.427	4.583 ± 0.307	0.300 ± 0.009	135	0.0	5
−2.55	1.303 ± 0.145	3.653 ± 0.257	2.770 ± 0.277	4.816 ± 0.196	0.312 ± 0.005	135	0.0	5
−1.08	1.613 ± 0.139	3.580 ± 0.248	2.704 ± 0.267	4.740 ± 0.189	0.309 ± 0.005	135	0.0	5
0.11	1.499 ± 0.141	3.574 ± 0.253	2.663 ± 0.261	4.796 ± 0.209	0.322 ± 0.005	135	0.0	5
1.31	1.330 ± 0.145	3.627 ± 0.257	2.746 ± 0.278	4.791 ± 0.196	0.321 ± 0.005	135	0.0	5
2.78	1.410 ± 0.164	3.586 ± 0.271	2.730 ± 0.295	4.711 ± 0.202	0.315 ± 0.007	135	0.0	5
5.08	1.004 ± 0.257	3.184 ± 0.438	2.265 ± 0.456	4.477 ± 0.329	0.310 ± 0.010	135	0.0	5
9.56	1.371 ± 0.416	3.309 ± 0.754	2.377 ± 0.762	4.607 ± 0.622	0.281 ± 0.013	135	0.0	5

TABLE 6—*Continued*

r (arcsec)	Hβ (Å)	[MgFe] (Å)	$\langle$Fe$\rangle$ (Å)	Mg b (Å)	Mg_2 (mag)	P.A. (deg)	Offset (arcsec)	Run
			GMP 3414					
−6.88	3.114 ± 0.797	4.175 ± 1.204	3.861 ± 1.256	4.515 ± 1.135	0.218 ± 0.036	178	4.6	3
−2.47	2.941 ± 0.467	4.273 ± 0.715	3.946 ± 0.734	4.628 ± 0.687	0.205 ± 0.015	178	4.6	3
1.56	3.037 ± 0.443	4.040 ± 0.742	3.466 ± 0.728	4.710 ± 0.741	0.275 ± 0.019	178	4.6	3
6.01	3.999 ± 0.642	3.195 ± 0.992	2.692 ± 1.002	3.791 ± 0.943	0.290 ± 0.021	178	4.6	3
−2.99	0.944 ± 0.318	3.357 ± 0.463	2.694 ± 0.492	4.183 ± 0.389	0.206 ± 0.011	88	0.0	3
−1.25	1.872 ± 0.125	3.448 ± 0.196	2.751 ± 0.198	4.321 ± 0.182	0.233 ± 0.004	88	0.0	3
−0.41	1.700 ± 0.103	3.425 ± 0.160	2.798 ± 0.162	4.193 ± 0.149	0.260 ± 0.003	88	0.0	3
0.20	1.342 ± 0.097	3.444 ± 0.151	2.853 ± 0.153	4.156 ± 0.141	0.269 ± 0.003	88	0.0	3
0.81	1.261 ± 0.121	3.346 ± 0.185	2.689 ± 0.186	4.164 ± 0.173	0.259 ± 0.004	88	0.0	3
1.65	1.680 ± 0.132	3.371 ± 0.211	2.508 ± 0.208	4.531 ± 0.192	0.254 ± 0.004	88	0.0	3
3.27	2.480 ± 0.290	2.956 ± 0.484	1.928 ± 0.454	4.532 ± 0.418	0.246 ± 0.009	88	0.0	3
			GMP 3958					
−2.94	2.359 ± 0.408	2.905 ± 0.738	2.720 ± 0.741	3.102 ± 0.686	0.221 ± 0.015	12	0.0	4
−1.82	1.712 ± 0.302	...	2.516 ± 0.508	...	...	12	0.0	4
−0.89	1.519 ± 0.220	...	2.350 ± 0.372	...	...	12	0.0	4
0.03	2.135 ± 0.196	...	2.298 ± 0.322	...	...	12	0.0	4
0.96	1.605 ± 0.198	2.873 ± 0.150	2.351 ± 0.331	3.510 ± 0.314	0.274 ± 0.007	12	0.0	4
1.88	2.270 ± 0.319	3.164 ± 0.406	2.479 ± 0.560	4.039 ± 0.458	0.268 ± 0.012	12	0.0	4
3.00	0.768 ± 0.399	3.332 ± 0.671	2.695 ± 0.650	4.120 ± 0.620	0.260 ± 0.015	12	0.0	4
			GMP 4822					
−5.69	1.462 ± 0.295	3.402 ± 0.489	2.760 ± 0.540	4.193 ± 0.386	0.271 ± 0.011	15	0.0	5
−2.77	1.226 ± 0.138	3.542 ± 0.235	2.691 ± 0.237	4.663 ± 0.208	0.290 ± 0.005	15	0.0	5
−1.34	1.561 ± 0.090	3.608 ± 0.156	2.726 ± 0.167	4.776 ± 0.120	0.311 ± 0.003	15	0.0	5
−0.47	1.751 ± 0.095	3.498 ± 0.155	2.560 ± 0.164	4.779 ± 0.116	0.335 ± 0.003	15	0.0	5
0.14	1.490 ± 0.084	3.627 ± 0.150	2.630 ± 0.158	5.001 ± 0.113	0.336 ± 0.003	15	0.0	5
0.75	1.501 ± 0.097	3.715 ± 0.160	2.839 ± 0.171	4.862 ± 0.126	0.334 ± 0.003	15	0.0	5
1.61	1.530 ± 0.101	3.638 ± 0.173	2.808 ± 0.187	4.713 ± 0.135	0.329 ± 0.004	15	0.0	5
3.06	1.244 ± 0.132	3.462 ± 0.226	2.596 ± 0.230	4.618 ± 0.193	0.313 ± 0.005	15	0.0	5
6.00	1.931 ± 0.240	3.466 ± 0.421	2.574 ± 0.448	4.667 ± 0.321	0.296 ± 0.009	15	0.0	5
			GMP 4928					
−3.64	1.248 ± 0.331	4.128 ± 1.160	3.215 ± 0.844	5.301 ± 0.666	0.277 ± 0.017	108	0.0	2
−1.38	1.096 ± 0.203	4.375 ± 0.424	3.807 ± 0.568	5.029 ± 0.341	0.316 ± 0.010	108	0.0	2
0.05	1.370 ± 0.142	4.382 ± 0.238	3.498 ± 0.372	5.488 ± 0.292	0.320 ± 0.007	108	0.0	2
1.48	0.908 ± 0.161	3.775 ± 0.187	2.859 ± 0.399	4.985 ± 0.249	0.317 ± 0.008	108	0.0	2
3.75	2.386 ± 0.292	3.478 ± 0.845	3.398 ± 0.791	3.559 ± 0.615	0.296 ± 0.015	108	0.0	2
−4.56	1.667 ± 0.427	3.742 ± 0.775	3.440 ± 0.789	4.070 ± 0.752	0.230 ± 0.019	108	0.0	3
−2.03	1.641 ± 0.198	3.196 ± 0.367	2.377 ± 0.369	4.298 ± 0.319	0.259 ± 0.006	108	0.0	3
−0.60	1.199 ± 0.171	3.708 ± 0.317	2.888 ± 0.321	4.760 ± 0.285	0.277 ± 0.007	108	0.0	3
0.57	1.268 ± 0.139	3.772 ± 0.255	2.988 ± 0.262	4.762 ± 0.226	0.286 ± 0.004	108	0.0	3
2.00	1.037 ± 0.212	3.746 ± 0.376	3.230 ± 0.389	4.344 ± 0.349	0.283 ± 0.008	108	0.0	3
4.52	1.137 ± 0.366	3.433 ± 0.665	2.597 ± 0.671	4.538 ± 0.584	0.256 ± 0.011	108	0.0	3
−3.40	0.403 ± 0.248	3.682 ± 0.558	2.974 ± 0.619	4.559 ± 0.490	0.270 ± 0.013	153	0.0	2
−2.45	1.476 ± 0.126	3.388 ± 0.132	2.540 ± 0.312	4.520 ± 0.249	0.282 ± 0.007	153	0.0	2
−1.58	2.145 ± 0.129	3.420 ± 0.144	2.488 ± 0.326	4.699 ± 0.259	0.286 ± 0.007	153	0.0	2
−0.97	2.032 ± 0.091	3.850 ± 0.084	3.015 ± 0.236	4.915 ± 0.186	0.290 ± 0.005	153	0.0	2
−0.37	1.544 ± 0.091	3.719 ± 0.078	2.929 ± 0.230	4.722 ± 0.183	0.289 ± 0.005	153	0.0	2
0.24	1.600 ± 0.096	3.675 ± 0.082	2.571 ± 0.225	5.253 ± 0.199	0.295 ± 0.005	153	0.0	2
0.85	1.438 ± 0.121	3.257 ± 0.110	2.418 ± 0.289	4.388 ± 0.234	0.299 ± 0.006	153	0.0	2
1.71	1.390 ± 0.127	3.577 ± 0.131	2.571 ± 0.294	4.978 ± 0.249	0.311 ± 0.007	153	0.0	2
2.93	0.902 ± 0.191	3.114 ± 0.266	2.366 ± 0.460	4.098 ± 0.371	0.292 ± 0.010	153	0.0	2
			GMP 5279					
−9.26	1.396 ± 0.455	2.751 ± 0.702	2.559 ± 0.884	2.958 ± 0.577	0.190 ± 0.013	146	0.0	1
−2.78	1.711 ± 0.152	3.729 ± 0.112	3.023 ± 0.309	4.599 ± 0.194	0.282 ± 0.004	146	0.0	1
−0.69	1.805 ± 0.121	3.781 ± 0.072	3.035 ± 0.246	4.711 ± 0.154	0.304 ± 0.004	146	0.0	1
0.64	1.473 ± 0.125	4.379 ± 0.090	3.765 ± 0.257	5.092 ± 0.160	0.303 ± 0.004	146	0.0	1
2.64	1.163 ± 0.146	3.872 ± 0.102	3.119 ± 0.289	4.808 ± 0.183	0.281 ± 0.004	146	0.0	1
8.38	2.002 ± 0.509	3.274 ± 1.016	2.899 ± 0.971	3.696 ± 0.639	0.211 ± 0.016	146	0.0	1

TABLE 6—*Continued*

r (arcsec)	Hβ (Å)	[MgFe] (Å)	$\langle$Fe$\rangle$ (Å)	Mg b (Å)	Mg_2 (mag)	P.A. (deg)	Offset (arcsec)	Run
			GMP 5568					
−4.60	1.301 ± 0.251	3.357 ± 0.485	2.650 ± 0.597	4.252 ± 0.484	0.278 ± 0.013	78	2.8	2
−2.05	0.972 ± 0.153	3.676 ± 0.201	2.897 ± 0.368	4.665 ± 0.297	0.306 ± 0.008	78	2.8	2
−0.60	1.532 ± 0.122	4.007 ± 0.143	3.307 ± 0.298	4.855 ± 0.240	0.312 ± 0.006	78	2.8	2
0.58	1.483 ± 0.115	3.435 ± 0.080	2.465 ± 0.229	4.787 ± 0.204	0.283 ± 0.005	78	2.8	2
2.03	0.982 ± 0.160	3.390 ± 0.186	2.470 ± 0.365	4.651 ± 0.300	0.276 ± 0.008	78	2.8	2
4.57	1.210 ± 0.254	3.248 ± 0.446	2.769 ± 0.559	3.811 ± 0.491	0.239 ± 0.012	78	2.8	2
−4.88	3.543 ± 0.527	3.731 ± 1.230	2.546 ± 1.265	5.468 ± 0.889	0.287 ± 0.026	78	14.0	5
−1.26	1.359 ± 0.674	4.238 ± 1.447	3.016 ± 1.515	5.956 ± 1.074	0.299 ± 0.032	78	14.0	5
2.66	3.033 ± 0.520	3.310 ± 1.386	1.987 ± 1.333	5.516 ± 0.915	0.283 ± 0.025	78	14.0	5
6.29	1.979 ± 0.871	3.692 ± 1.847	3.079 ± 2.072	4.427 ± 1.450	0.286 ± 0.042	78	14.0	5
−4.08	0.434 ± 0.271	3.096 ± 0.468	2.619 ± 0.605	3.661 ± 0.500	0.248 ± 0.014	168	0.0	2
−2.20	1.313 ± 0.135	3.768 ± 0.157	2.752 ± 0.321	5.157 ± 0.260	0.265 ± 0.007	168	0.0	2
−1.36	1.300 ± 0.145	3.798 ± 0.152	2.826 ± 0.303	5.103 ± 0.265	0.268 ± 0.006	168	0.0	2
−0.75	1.373 ± 0.089	3.643 ± 0.065	2.680 ± 0.210	4.952 ± 0.171	0.280 ± 0.005	168	0.0	2
−0.14	1.343 ± 0.079	3.845 ± 0.050	3.013 ± 0.172	4.908 ± 0.152	0.287 ± 0.004	168	0.0	2
0.46	1.272 ± 0.095	3.868 ± 0.083	2.895 ± 0.231	5.170 ± 0.186	0.296 ± 0.005	168	0.0	2
1.07	1.405 ± 0.126	3.408 ± 0.112	2.477 ± 0.306	4.688 ± 0.214	0.290 ± 0.006	168	0.0	2
1.91	0.810 ± 0.157	3.340 ± 0.176	2.373 ± 0.359	4.701 ± 0.294	0.300 ± 0.008	168	0.0	2
3.80	1.333 ± 0.302	2.913 ± 0.549	2.053 ± 0.677	4.135 ± 0.557	0.265 ± 0.016	168	0.0	2
−3.77	1.503 ± 0.412	3.354 ± 0.730	2.504 ± 0.781	4.492 ± 0.553	0.257 ± 0.016	168	0.0	5
−2.31	1.677 ± 0.253	3.380 ± 0.423	2.495 ± 0.447	4.579 ± 0.325	0.265 ± 0.009	168	0.0	5
−1.47	1.583 ± 0.229	3.710 ± 0.400	2.729 ± 0.424	5.043 ± 0.304	0.274 ± 0.009	168	0.0	5
−0.86	1.564 ± 0.228	3.605 ± 0.386	2.713 ± 0.423	4.792 ± 0.279	0.280 ± 0.008	168	0.0	5
−0.26	1.631 ± 0.193	3.900 ± 0.333	2.901 ± 0.356	5.242 ± 0.251	0.295 ± 0.007	168	0.0	5
0.35	1.575 ± 0.202	3.671 ± 0.378	2.692 ± 0.392	5.005 ± 0.302	0.275 ± 0.006	168	0.0	5
0.96	1.295 ± 0.242	3.647 ± 0.425	2.512 ± 0.433	5.294 ± 0.320	0.274 ± 0.009	168	0.0	5
1.80	1.881 ± 0.296	3.624 ± 0.566	2.404 ± 0.569	5.465 ± 0.415	0.268 ± 0.011	168	0.0	5
3.50	1.687 ± 0.552	3.326 ± 0.907	2.467 ± 0.973	4.485 ± 0.678	0.264 ± 0.020	168	0.0	5
			GMP 5975					
−8.13	0.863 ± 0.450	2.885 ± 0.628	2.432 ± 0.692	3.421 ± 0.515	0.195 ± 0.013	68	0.0	5
−3.89	1.553 ± 0.211	3.078 ± 0.310	2.724 ± 0.346	3.479 ± 0.259	0.211 ± 0.008	68	0.0	5
−2.01	1.724 ± 0.140	3.392 ± 0.210	2.855 ± 0.227	4.029 ± 0.179	0.215 ± 0.004	68	0.0	5
−1.17	1.766 ± 0.102	3.488 ± 0.161	2.833 ± 0.176	4.294 ± 0.130	0.249 ± 0.004	68	0.0	5
−0.57	1.671 ± 0.084	3.508 ± 0.136	2.787 ± 0.150	4.414 ± 0.105	0.298 ± 0.003	68	0.0	5
0.04	1.609 ± 0.071	3.539 ± 0.114	2.796 ± 0.124	4.479 ± 0.091	0.316 ± 0.003	68	0.0	5
0.65	1.767 ± 0.082	3.534 ± 0.131	2.812 ± 0.140	4.440 ± 0.109	0.307 ± 0.003	68	0.0	5
1.25	1.749 ± 0.105	3.561 ± 0.165	2.920 ± 0.180	4.343 ± 0.134	0.290 ± 0.004	68	0.0	5
2.09	1.594 ± 0.263	3.512 ± 0.388	2.995 ± 0.431	4.119 ± 0.318	0.279 ± 0.010	68	0.0	5
3.99	1.824 ± 0.193	3.183 ± 0.311	2.667 ± 0.346	3.800 ± 0.250	0.246 ± 0.007	68	0.0	5
7.82	1.413 ± 0.431	2.760 ± 0.645	2.381 ± 0.699	3.200 ± 0.555	0.248 ± 0.017	68	0.0	5

NOTE.—Table 6 is also available in machine-readable form in the electronic edition of the *Supplement*.

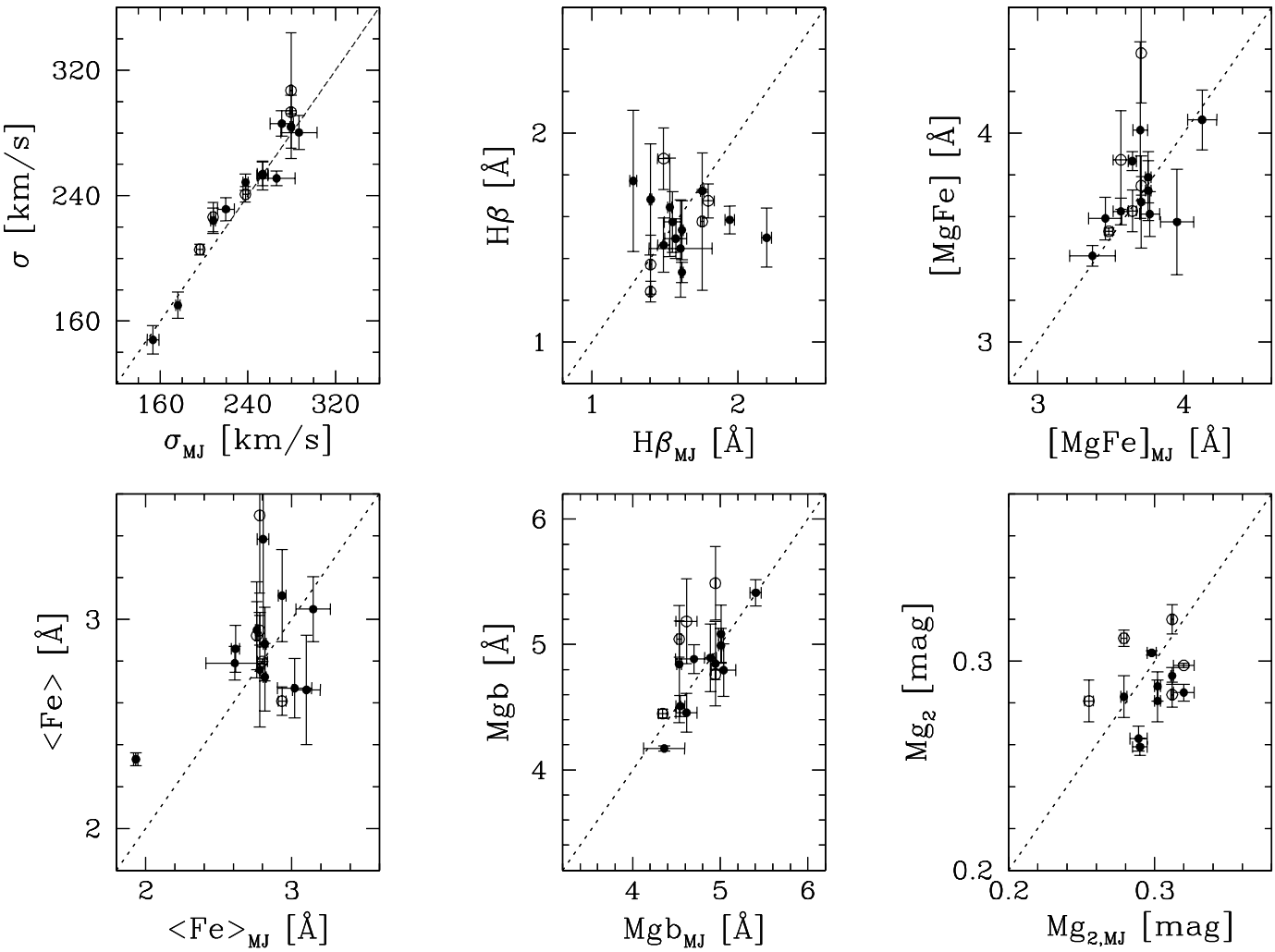

FIG. 7.—Central values of σ, Hβ, [MgFe], $\langle$Fe$\rangle$, Mg b, and Mg_2 measured within an aperture of 2″ along the minor (*filled circles*) and diagonal axes (*open circles*) are compared to those measured in Paper I along the major axis.

two data sets are in agreement within the errors. Figure 7 shows the central values of σ, Hβ, [MgFe], $\langle$Fe$\rangle$, Mg b, and Mg_2 obtained along the minor and diagonal axes of the sample galaxies as a weighted mean of the values available within an aperture of 2″ and those obtained along the corresponding major axes. Most of the data are consistent within 3 σ errors. No systematic effects are observed for the remaining ones.

5. CONCLUSIONS

New radially resolved spectroscopy of 12 E and S0 galaxies of the Coma Cluster was presented. The rotation curves, velocity dispersion profiles, and the H_3 and H_4 coefficients of the Hermite decomposition of the line-of-sight velocity distribution were derived along the minor axis, offset major axis, and one diagonal direction. Moreover, the line strength index profiles of Mg, Fe, and Hβ line indices were measured too. In addition, the surface photometry of the central regions of a subsample of four galaxies recently obtained with *HST* WFPC2 was presented.

The data complement the existing set (Paper I, Paper II) and have a precision and radial extent sufficient to construct flattened and rotating dynamical models of the galaxies and study their radially resolved stellar populations. Other papers address these issues (Paper III; Thomas et al. 2005, 2007).

E. M. C. acknowledges the Max-Planck-Institut für extraterrestrische Physik for hospitality while this paper was in progress. E. M. C. receives support from grant PRIN2005/32 by Istituto Nazionale di Astrofisica (INAF) and from grant CPDA068415/06 by the Padua University. This work was supported by the Sonderforschungsbereich 375 "Astro-Teilchenphysik" of the Deutsche Forschungsgemeinschaft. Support for program HST-GO-10884.0-A was provided by NASA through a grant from the Space Telescope Science Institute, which is operated by the Association of Universities for Research in Astronomy, Inc., under NASA contract NAS5-26555.

REFERENCES

Bender, R. 1990, A&A, 229, 441
Bender, R., & Möllenhoff, C. 1987, A&A, 177, 71
Bender, R., Saglia, R. P., & Gerhard, O. E. 1994, MNRAS, 269, 785
Faber, S. M., Friel, E. D., Burstein, D., & Gaskell, C. M. 1985, ApJS, 57, 711
Gerhard, O. E. 1993, MNRAS, 265, 213
Gerhard, O., Kronawitter, A., Saglia, R. P., & Bender, R. 2001, AJ, 121, 1936
González, J. J. 1993, Ph.D. thesis, Univ. California
Gorgas, J., Efstathiou, G., & Aragon Salamanca, A. 1990, MNRAS, 245, 217
Holtzman, J. A., et al. 1995, PASP, 107, 156
Jørgensen, I., Franx, M., & Kjaergaard, P. 1995, MNRAS, 276, 1341

Kent, S. M., & Gunn, J. E. 1982, AJ, 87, 945
Mehlert, D., Saglia, R. P., Bender, R., & Wegner, G. 1998, A&A, 332, 33
———. 2000, A&AS, 141, 449 (Paper I)
Mehlert, D., Thomas, D., Saglia, R. P., Bender, R., & Wegner, G. 2003, A&A, 407, 423 (Paper III)
Osterbrock, D. E. 1989, Astrophysics of Gaseous Nebulae and Active Galactic Nuclei (Mill Valley: University Science)
Osterbrock, D. E., Fulbright, J. P., Martel, A. R., Keane, M. J., Trager, S. C., & Basri, G. 1996, PASP, 108, 277
Shetrone, M., et al. 2007, PASP, 119, 556
Thomas, D., Maraston, C., & Bender, R. 2003, MNRAS, 339, 897
Thomas, J. 2006, Ph.D. thesis, Ludwig Maximillian Univ., Munich
Thomas, J., Saglia, R. P., Bender, R., Thomas, D., Gebhardt, K., Magorrian, J., Corsini, E. M., & Wegner, G. 2007, MNRAS, 382, 657
———. 2005, MNRAS, 360, 1355
Thomas, J., Saglia, R. P., Bender, R., Thomas, D., Gebhardt, K., Magorrian, J., & Richstone, D. 2004, MNRAS, 353, 391
van der Marel, R. P., & Franx, M. 1993, ApJ, 407, 525
Wegner, G., Corsini, E. M., Saglia, R. P., Bender, R., Merkl, D., Thomas, D., Thomas, J., & Mehlert, D. 2002, A&A, 395, 753 (Paper II)
Worthey, G., Faber, S. M., Gonzalez, J. J., & Burstein, D. 1994, ApJS, 94, 687